



Gonçalo Nuno Fernandes Ritto

Licenciado em Engenharia de Micro e Nanotecnologias

Growing of biomorphic nanomaterials based on calcium carbonate

Dissertação para Obtenção do Grau de Mestre em
Engenharia de Micro e Nanotecnologias

Orientador: Isabel Maria Mercês Ferreira, Professora Associada,
Faculdade de Ciências e Tecnologia da UNL

Co-orientadores: Ana Baptista, Investigadora de Pós-Doutoramento
Faculdade de Ciências e Tecnologia da UNL

Júri

Presidente: Rodrigo Ferrão de Paiva Martins, Professor Catedrático,
Faculdade de Ciências e Tecnologia da UNL

Arguente: João Paulo Miranda Ribeiro Borges, Professor Auxiliar,
Faculdade de Ciências e Tecnologia da UNL

Vogal: Isabel Maria Mercês Ferreira, Professora Associada,
Faculdade de Ciências e Tecnologia da UNL

Novembro de 2016

[Verso da Capa]

Crescimento de Nanomateriais Biomorficos à base de carbonato de cálcio

Copyright © Gonçalo Nuno Fernandes Ritto, Faculdade de Ciências e Tecnologia, Universidade Nova de Lisboa.

A Faculdade de Ciências e Tecnologia e a Universidade Nova de Lisboa têm o direito, perpétuo e sem limites geográficos, de arquivar e publicar esta dissertação através de exemplares impressos reproduzidos em papel ou de forma digital, ou por qualquer outro meio conhecido ou que venha a ser inventado, e de a divulgar através de repositórios científicos e de admitir a sua cópia e distribuição com objetivos educacionais ou de investigação, não comerciais, desde que seja dado crédito ao autor e editor.

Agradecimentos

Agradeço a todos as pessoas que me ajudaram a chegar até aqui.

Agradeço principalmente à minha orientadora de tese, professora Isabel Ferreira, por me ter dado a oportunidade de desenvolver este tema, por todos os ensinamentos, paciência, e pelo tempo gasto e despesas monetárias comigo.

Agradeço também à Ana Baptista, Inês Ropio, David Sousa, Paulo Duarte, Catarina Marques e a todas as outras pessoas do Departamento, que me deram a sua ajuda para conseguir fazer este trabalho.

Agradeço também ao Departamento de Conservação e Restauro por me ter disponibilizado o microscópio Raman.

Agradeço aos meus colegas de curso, tanto pela companhia como pela ajuda que me deram no laboratório.

Agradeço também à minha família e amigos que me apoiaram durante todo este percurso.

This work was possible due to the partial financing support of the following projects: H2020-ICT-2014-1, RIA, TransFlexTeg-645241; ERC-CoG-2014, ChapTherPV, 647596; and by FEDER funds through the COMPETE 2020 Program and National Funds through FCT - Portuguese Foundation for Science and Technology under the project UID/CTM/50025/2013.

Resumo

Neste trabalho foi produzido carbonato de cálcio por precipitação: banho de óleo e ultra sons, onde vários parâmetros foram testados: temperatura, velocidade de agitação magnética, concentração dos reagentes, duração da reação e meio da reação. Algumas amostras ficaram em repouso durante um mês antes de algum precipitado ser removido, lavado e seco para a caracterização do pó sem este ter nenhum produto secundário ou solvente da reação.

A técnica de “dip-coating” foi utilizada para produzir carbonato de cálcio com uma matriz orgânica (PVP – Polyvinylpyrrolidone) numa tentativa de produzir nacre artificial. Vários parâmetros foram testados: número de ciclos, temperatura, tempo de imersão e de secagem; presença/falta de uma etapa intermédia e velocidade de imersão.

Dois polimorfos anidros do carbonato de cálcio foram produzidos por ambos os métodos: vaterite e calcite.

Algumas amostras foram caracterizadas por DRX (Difração por raios-X), Espectroscopia Raman e foram analisadas por SEM (Microscópio Eletrónico de Varrimento).

Espectrofotometria foi também utilizada para ver a diferença da absorvância/transmitância e refletância de algumas amostras de “dip-coating”. As amostras com uma matriz orgânica mostraram uma transmitância muito elevada na região do infra-vermelho e uma baixa transmitância na região do visível ao contrário das amostras com apenas camadas inorgânicas indicando a possibilidade da formação de um complexo orgânico/inorgânico.

Palavras-chave: Carbonato de cálcio; síntese química; “dip-coating”, Nacre

Abstract

Calcium carbonate was produced by precipitation: oil bath and ultra-sounds, being studied several parameters such as: temperature, magnetic stir speed, concentration of the reagents, duration of the reaction and the medium of the reaction. Samples rested for a month before some of the precipitated was removed, washed and dried to get the powder characterized without any secondary product or the solvent of the reaction.

Dip-coating technique was also used to produce calcium carbonate with an organic matrix (PVP - Polyvinylpyrrolidone) in an attempt to produce artificial nacre. Several parameters were also modified: number of coating cycles, temperature, dip and dry time; presence/absence of an in-between step and dipping speed.

Two anhydrous polymorphs of calcium carbonate were produced from both methods: vaterite and calcite.

Some samples were characterized by XRD (X-ray Diffraction), Raman Spectroscopy and were analysed by SEM (Scanning Electron Microscopy).

Spectrophotometry was also used to analyse the absorbance/transmittance and reflectance of some dip-coated samples. The samples with an organic matrix showed a very high transmittance in the infra-red region and a very low transmittance in the visible region unlike samples with just inorganic layers indicating the possibility of formation of an organic/inorganic complex.

Keywords: Calcium carbonate, chemical synthesis, dip-coating, Nacre

Index

Agradecimientos	v
Resumo	vii
Abstract	ix
Index	xi
Table Index	xiii
Figure Index	xv
Objective	1
1 Introduction	2
1.1 Calcium carbonate	2
1.2 Applications	3
1.3 Nacre	4
2 Materials and Methods	6
2.1 Synthesis	6
2.2 Characterization	7
3 Results and discussion	8
3.1 Synthesis of CaCO ₃ by precipitation	8
3.2 Influence of solution's temperature, magnetic stirring speed and reaction time	9
3.3 Structural and morphologic analysis	9
3.4 Purified calcium carbonate powders.....	21
3.5 Synthesis of CaCO ₃ films by Dip-Coating	24
4 Conclusions and future perspectives	29
References	31
Annex	39
Annex 1	40
Annex 2	43
Annex 3	49

Table Index

Table A1. 1: Solution parameters tested.....	40
Table A1. 2: Dip-coating parameters used	41
Table A2. 1: Influence of time and temperature for a solution with magnetic stir at 400rpm.....	43
Table A2. 2: Influence of time and temperature for a solution with magnetic stir at 800rpm.....	44
Table A2. 3: Influence of time and temperature for a solution without magnetic stir. ..	46
Table A2. 4: Influence of the ultra-sounds in the solution	48
Table A3. 1: Influence of dip parameters and dip cycles in the transmittance of samples with the respective images of films taken in the microscope.....	49

Figure Index

Figure 1 - Calcium carbonate crystals in nature, from left to right: Aragonite[9]; Vaterite[10]; Calcite[11].....	2
Figure 2 - Different literature images exemplifying: amorphous calcium carbonate (ACC, a); ACC and vaterite nanoaggregates (b, c); and vaterite nanoaggregates (d, e). Pictures at the bottom correspond to: vaterite nanoaggregates and first calcite crystals (f); calcite crystals attached to vaterite spheres with the development of growth steps on the calcite surface (g); calcite growth steps and vaterite nanoparticulate subunits (h) and calcite crystals with vaterite casts (i).[13].....	3
Figure 3 - Scheme of layers of nacre in the outer layer of a pearl[32] ; Interior of a nautilus shell which contains the iridescent nacre[33]	4
Figure 4 - Heating plate, Heidolph	6
Figure 5 - Ultra-sonic machine, (Sonorex, Bandelin)	6
Figure 6 - Images of SEM and optical microscopy for samples synthesized during 60 minutes at 40°C at 400 rpm and 800rpm magnetic stir. a) Optical microscopy of crystals at 400 rpm. b) Optical microscopy of crystals at 800 rpm. c) SEM image of crystals at 400 rpm. d) SEM image of crystals at 800 rpm.	10
Figure 7- a) – Micro Raman Spectra of samples prepared during 60 min and at 40°C with a different magnetic stir speed b) XRD pattern of samples synthesized at 40°C during 60min with a different rotation speed	11
Figure 8 - Images of SEM and optical microscopy for samples synthesized at 40°C and 75°C. a) Optical microscopy of crystals at 40°C; b) Optical microscopy of crystals at 75°C; c) SEM image of crystals at 40°C; d) SEM image of crystals at 75°C.....	13
Figure 9 - Samples synthesized during 60 min at 400 rpm with different temperatures: a) Raman spectra; b) XRD pattern.	14
Figure 10 - Images of SEM and optical microscopy for samples synthesized at different reaction times: a) SEM image of crystals at 5 minutes reaction time; b) Optical microscope image of crystals at 5 minutes reaction time; c) SEM image of crystals at 30 minutes reaction time; d) Optical microscope image of crystals at 30 minutes reaction time; e) SEM image of crystals at 60 minutes reaction time; f) Optical microscope image of crystals at 60 minutes reaction time; g) SEM image of crystals at 24 hours reaction time; h) Optical microscope image of crystals at 24 hours reaction time.	16

Figure 11 - Samples synthesized at 400 rpm and 40°C at different reaction time: a) Micro Raman spectra; b) XRD pattern.....	17
Figure 12 - Microscopy and SEM images of samples synthesized at 40°C during 30 minutes for magnetic stir of 400 rpm varying CaCl ₂ *2H ₂ O:NaHCO ₃ ratios; a) SEM image of (1:1 ratio); b) Optical microscope image of (1:1 ratio); c) SEM image of (1:2 ratio); d) Optical microscope image of (1:2 ratio); e) SEM image of (1:4 ratio); f) Optical microscope image of (1:4 ratio); g) SEM image of (1:6 ratio); h) Optical microscope image of (1:6 ratio).	18
Figure 13 - Microscopy and SEM images of samples synthesized at 75°C during 30 minutes for magnetic stir at 400 rpm varying CaCl ₂ *2H ₂ O:NaHCO ₃ ratios: a) SEM image of (1:4 ratio); b) Optical microscope image of (1:4 ratio); c) SEM image of (1:5 ratio); d) Optical microscope image of (1:5 ratio)	19
Figure 14 - a) Micro Raman spectra of 4 samples synthesized during 30 minutes at 40°C at 400 RPM with different reagents (CaCl ₂ *2H ₂ O/(NaHCO ₃) ₂) ratios. b) Micro Raman spectra of 2 samples synthesized during 30 minutes at 75°C at 400 rpm with different reagents (CaCl ₂ *2H ₂ O/(NaHCO ₃) ₂) ratios. c) XRD pattern of 4 samples synthesized during 30 minutes at 40°C at 400 RPM with different reagents (CaCl ₂ *2H ₂ O/(NaHCO ₃) ₂) ratios.	21
Figure 15 - SEM, microscopy and EDS images of samples washed after preparation: a) SEM image of crystals at 120 minutes 75°C 400 rpm; b) Optical microscope image of crystals at 120 minutes 75°C 400 rpm; c) SEM image of crystals at 120 minutes 40°C 400 rpm; d) Optical microscope image of crystals at 120 minutes 40°C 400 rpm; e) SEM image of crystals at 120 minutes 40°C 800 rpm; f) Optical microscope image of crystals at 120 minutes 40°C 800 rpm; g) SEM image of crystals at 60 minutes 75°C 800 rpm; h) Optical microscope image of crystals at 60 minutes 75°C 800 rpm; i) EDS spectrum of the sample at 60 minutes 75°C 800 rpm.....	23
Figure 16- a) Micro Raman spectra and b) XRD pattern of samples washed after synthesis: i. 120 min 75° and 400rpm; ii. 120 min 40° and 400rpm; iii. 120 min 40° and 800rpm and; iv. 60 min, 75° and 800rpm.....	24
Figure 17 - Absorbance at 1500 nm versus number of cycles varying the dip time keeping constant T=40°C and 3 min Dry.	25
Figure 18 - Absorbance as a function of the number of cycles at 500 nm for different sequences; cycle of 2min dip in the PVP, and 3 min dry for a dip speed 5mm/s, ambient temperature of 27°C and 10 seconds of dip time in the inorganic reagents.	26

Figure 19 - a) Absorbance and b) reflectance as a function of the wavelength for different sequences of cups at 10 cycles; cycle of 2min dip in the organic cup, and 3 min dry for a dip speed 5mm/s, ambient temperature of 27°C and 10 seconds of dip time in the inorganic reagents..... 27

Figure 20 - a) and b) SEM images of the dip coated samples respectively for 20 cycles, T amb(27°C), 1 min dip, acetone and 10 cycles, 40°C, 3 min dip; c) Raman spectra of dip-coated samples at 5 mm/s and 3 min dry time with different number of cycles, different temperature, different dip and with/without in-between cup, d) XRD pattern of sample dip- coated at ambient temperature and at 5 mm/s with cup of acetone dipped during 2 secs in-between the inorganic cups..... 28

Objective

The objective of this work was to find a facile synthesis process to grow nacre. In nature nacre is formed by alternate sheets of CaCO_3 with organic compound. To achieve this goal, the work performed in this thesis follows two approaches: first the synthesis of pure CaCO_3 was tried and then a layer-by-layer process using an automated dip-coating was used to growth CaCO_3 film directly into a glass substrate.

To achieve the synthesis of pure CaCO_3 , several parameters of the reaction were modified in order to know about its polymorphs. The changed parameters of the reaction were: temperature, time, stirring speed, different concentration of reagents and influence of the medium (oil bath or ultra-sounds). The reactants were CaCl_2 (calcium chloride) and NaHCO_3 (sodium bicarbonate) and the solvent was ethylene glycol ($\text{C}_2\text{H}_6\text{O}_2$).

The dip-coating technique was utilized in an attempt to produce nacre alternating between an organic and inorganic solution were several parameters varied such as temperature, dip and dry time, with/without in-between cup, number of cycles, dipping speed.

SEM (Scanning Electron Microscopy), XRD (X-ray Diffraction), Raman Spectroscopy and Spectrophotometry techniques supported the investigation performed.

1 Introduction

1.1 Calcium carbonate

Minerals have been produced for more than 3500 million years from different species of animals[1]. The biominerals are the inorganic phase formed in biological systems and widespread in nature. They have a hierarchical structure and special functions like the silica cell wall of the diatom, the calcitic spine of sea urchin, and the calcitic otolith of the marine algae. The process that leads to the formation of biominerals is called biomineralization. Calcium carbonate is one of the most important biominerals found in mammalian hard tissues[2]. Calcium carbonate have three anhydrous polymorphs: calcite, vaterite and aragonite (Figure 1) and 2 hydrated polymorphs: ikaite ($\text{CaCO}_3 \cdot 6\text{H}_2\text{O}$) and monohydrocalcite ($\text{CaCO}_3 \cdot \text{H}_2\text{O}$). There are also some amorphous calcium carbonate (ACC) with different degrees of short range order and degree of hydration[3]–[7]. It is extremely difficult to know about the formation of these polymorphs because there are many parameters involved in biomineralization.[8]



Figure 1 - Calcium carbonate crystals in nature, from left to right: Aragonite[9]; Vaterite[10]; Calcite[11]

Many efforts have been made in order to understand the biomineralization mechanisms. The metastable amorphous calcium carbonate is the first to be formed because it has the lowest free energy barrier.[8] ACC will then transform into aragonite and vaterite and then to calcite the most thermodynamically stable polymorph under ambient conditions.[12]

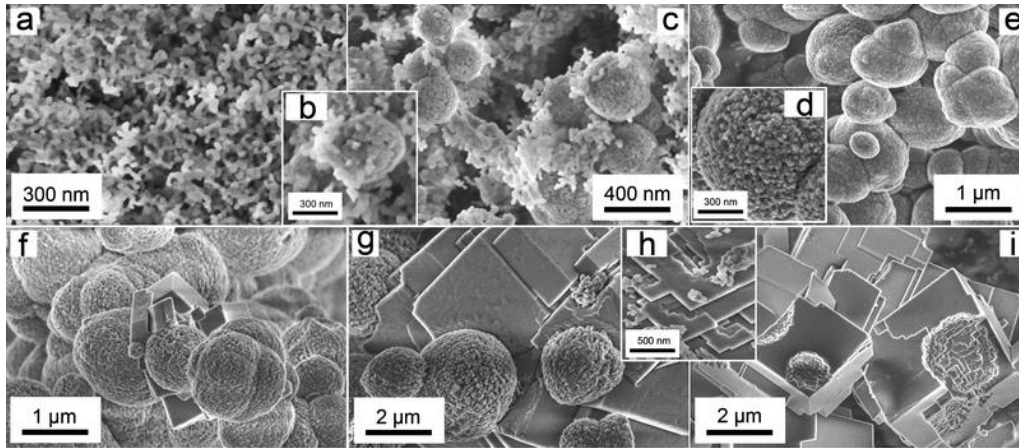


Figure 2 - Different literature images exemplifying: amorphous calcium carbonate (ACC, a); ACC and vaterite nanoaggregates (b, c); and vaterite nanoaggregates (d, e). Pictures at the bottom correspond to: vaterite nanoaggregates and first calcite crystals (f); calcite crystals attached to vaterite spheres with the development of growth steps on the calcite surface (g); calcite growth steps and vaterite nanoparticulate subunits (h) and calcite crystals with vaterite casts (i).[13]

Some findings of those researches were that with a higher CO₂ pressure and a pH between 8,5 and 10,5 favours the formation of vaterite but with lower CO₂ pressure and a pH around 7 and higher than 11 calcite is favored.[14][15][16][17]. Han et.al said that increasing Ca²⁺ ion concentration in a solution favours the appearance of calcite over vaterite.[18] To obtain aragonite the pH of the solution should be lower than 11, the temperature should be high and Magnesium present in the solution.[19]

Vaterite is the most unstable CaCO₃ polymorph and can be transformed into aragonite and calcite easily[20] and is the rarest polymorph in nature but it still can be found in: gallstones,[21] gastropods eggshells,[22] freshwater lackluster pearls,[23] in a member of the ascidians, the snail, carp otoliths and sea squirts. Vaterite formation is under strictly genetic control. Vaterite acts as a transient precursor or as functional component for structural purposes.[22] It has been stated that it is possible to transform calcite to vaterite too [23]. The lackluster pearls are made from vaterite crystals which change its mechanical and optical properties[24]. The good solubility of vaterite can make it a good material for applications in biomedical area.[25]

1.2 Applications

CaCO₃ has many applications in several materials: rubber, paint, imitation leather, soap, inorganic filler for plastic and paper.[26] CaCO₃ also has many potential applications in areas like pharmaceutical and medicine (drug-delivery) and ion exchange/absorption thanks to its properties such as biodegradability, bio-compatibility and pH sensitivity.[27][28][29]

CaCO_3 as other nano particles can change/improve their properties at submicron scale like: mechanical and optical properties, increased surface area, better barrier effects in a polymer matrix and better chemical reactivity.[30]

Submicron CaCO_3 particles are required to improve the rheology and the opacity of paints and coatings and also as a lubricant additive.[26]

With CaCO_3 being produced by a low-cost method it could be applied not only in a few applications but also replacing silica and titania by a bio-degradable material.[26]

1.3 Nacre

The elaborate properties of nacre come from the intricate structure at many scale levels between an organic matrix and calcium carbonate fibers and tablets[31] which can be seen in Figure 3.

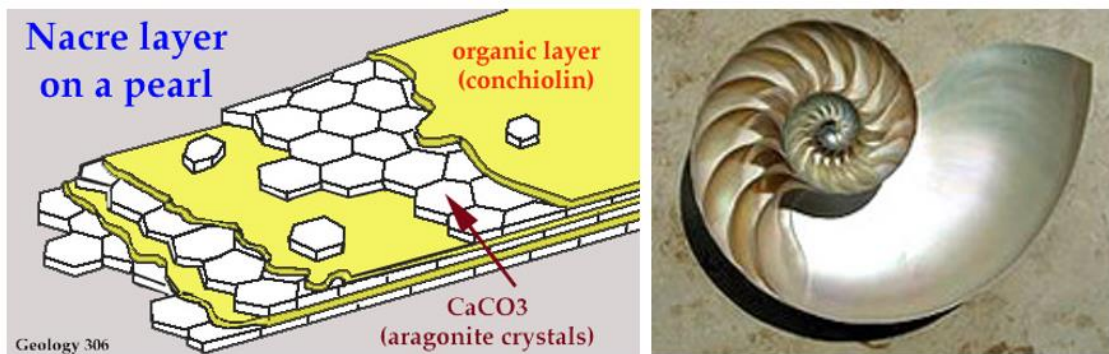


Figure 3 - Scheme of layers of nacre in the outer layer of a pearl[32] ; Interior of a nautilus shell which contains the iridescent nacre[33]

Nacre (Figure 3) and coral had attracted the attention of many orthopedists because they can replace some components used by them that exhibit toxicity, incompatibility and mechanical strength problems.

The nacre has very good mechanical properties, in particular the hardness. This makes the nacre a good candidate to be applied in hardened synthetic ceramics. [34]

Nacre is 3000 times stronger than its components individually thanks to the organic matrix that dissipates the tension and the crystals shapes and sizes. [35]

Nacre has a very high elastic modulus compared to bulk CaCO_3 aragonite phase. Several studies with nacre were conducted: like treat myopia of chicks[36], induce osteogenesis in

vitro[37] and in the vertebrae of sheep[38], induce cutaneous fibroblast growth in rats[39]. It gathered much attention by scientist whom try to reproduce the structure of nacre [40]. There is a group of researchers who could produce artificial nacre. [41] It is not easy to control the formation of a specific phase of CaCO_3 artificially[42] but in nature, animals can produce aragonite inside the shell and calcite outside of it. There are some investigations about this selectivity of polymorphs, about the conditions of formation and the role of macromolecules and they suggest the existence of nanoclusters of ACC which are then transformed into the different polymorphs[43][44].

Many aspects in the role of organic matrix in the formation of the skeleton in corals are still enigmatic. Some experiences in vitro showed that the organic matrix have influence in the polymorph phase of the calcium carbonate.[45] They say that the Mediterranean zooxanthellate solitary coral, *Balanophyllia europaea*, can favor the precipitation of aragonite and stated that a transient amorphous calcium carbonate was stabilized by lipids is involvement.

The organic matrix of: *Acropora digitifera*, *Lophelia pertusa*, and *Montipora caliculata* macromolecules can influence the precipitation of the calcium carbonate too.[46]

Amino-acids are the building units of proteins and they have amino and carboxyl groups simultaneously. Amino-acids can regulate the nucleation, the growth, and the structures of the inorganic crystals.[47]

One recent study also said that four acidic proteins from the genes of *Stylophora pistillata* can catalyse spontaneously the precipitation of calcium carbonate from sea water.[48]

Valiyaveetil et al. isolated pelovaterin, a glycine-rich peptide from eggshells of a soft-shell turtle. In vitro tests showed that pelovaterin induce the formation of vaterite, modify the crystal morphology and increases their growth rate[49]

The organic/inorganic hybrid microstructure inspired people to create nacre like composites materials as: gas barriers, electric insulators, fire retardants buildings and furniture materials.[50]

2 Materials and Methods

2.1 Synthesis

The synthesis of CaCO_3 by precipitation was performed using the following quantities of reagents: $M(\text{CaCl}_2 \cdot 2\text{H}_2\text{O}) = 147 \text{ g/mol}$; $M(\text{NaHCO}_3) = 84 \text{ g/mol}$; $M(\text{C}_2\text{H}_6\text{O}_2) = 62.07 \text{ g/mol}$ in ethylene glycol leading to a mass of $m(\text{CaCl}_2 \cdot 2\text{H}_2\text{O}) = 147 \times 5 \times 10^{-3} = 735 \text{ mg}$ and $m(\text{NaHCO}_3) = 840 \text{ mg}$. A quantity of 5 mmol of dehydrated calcium chloride ($\text{CaCl}_2 \cdot 2\text{H}_2\text{O}$), Sigma Aldrich were dissolved in 50 mL ethylene glycol (99%, Sigma Aldrich) by ultra sounds bath for 2 hours at 40°C . Then 10 mmol of sodium bicarbonate (NaHCO_3) Ultra, Sigma Aldrich was dispersed in 50 mL of ethylene glycol by magnetic stirring overnight at 1100 rpm and at ambient temperature. Each flask was filled with 2.5 mL of ethylene glycol with (NaHCO_3) and 2.5 mL of ethylene glycol with $\text{CaCl}_2 \cdot 2\text{H}_2\text{O}$ to obtain a molar concentration of (1:2) ($\text{CaCl}_2 \cdot 2\text{H}_2\text{O}:\text{NaHCO}_3$). To obtain a solution with a molar concentration of (1:4) instead of a 2.5 ml solution of NaHCO_3 , it was added 5 ml of NaHCO_3 to the final solution. All the parameters tested are indicated in Table A1. 1 of annex 1.

The resulting dispersion was heated up for different times, from 5 minutes to 24 hours, different temperatures (40°C and 75°C), and for different methods (Ultra-sounds bath in the ultra-sounds machine (Sonorex, Bandelin) of Figure 5 at Lab 213, DCM, FCT-UNL and oil bath (baysilone oil M350 heated in a plate (Heildolph) that can be observed on Figure 4)) at Lab 213, DCM, FCT-UNL.



Figure 4 - Heating plate, Heidolph



Figure 5 - Ultra-sonic machine, (Sonorex, Bandelin)

For observation at the microscope a small quantity of the liquid was placed in a glass surface and heated up to 70°C in oven during approximately 2 hours to dry.

After preparation, some solutions samples rested for 1 month. The CaCO₃ nanoparticles were separated from the turbid product sol, by washing 4 times with a mixture of water and ethanol 200 µl (1:1) and by centrifugation at 9000 rpm during 20 minutes.

The different solutions were used in a dip-coater where a glass substrate was attached to pneumatic arm of the equipment, the glass was dipped for different parameters: temperature, dip and dry times, number of cycles, alternating with different reagents.

The main reagents were the same prepared for the synthesis of CaCO₃ by solution. In same experiences an in-between cup of water/acetone/PVP-methanol solution was used. All the combinations are presented in the table: Table A1. 2

The films produced by dip-coating were dried at ambient temperature during 2 days.

2.2 Characterization

The produced samples were characterized by observing its surface morphology in an inverted optical microscope (Leica DMI8, at Lab 213, DCM, FCT-UNL) and a representative selection of these samples were analysed also by a scanning electron microscope (SEM - Hitachi S2400 with Bruker light elements EDS, at MicroLab-Electron Microscopy Laboratory of *Instituto Superior Técnico*). For SEM analysis, the powder or glass coated samples were placed in the sample holder using a carbon ribbon and then covered with a very thin layer of gold.

The compositional/structural analysis was performed by Raman microscopy (Labram 300 Jobin Yvon spectrometer, equipped with a solid state laser operating at 532 nm, at Lab 217, *Departamento de Conservação e Restauro*, FCT UNL) and by X-ray diffraction (XRD - PANalytical X'Pert PRO equipped with an X'Celerator detector using CuK α radiation at 45 kV and 40 mA, in a Bragg–Brentano configuration. The analysis was performed over the angular 2 θ range 10°–80°, with a scanning step of 0.03° at CENIMAT-I3N, FCT-UNL.

The UV-VIS-NIR spectroscopy was performed in a JASCO V-770 spectrophotometer, for wavelengths in the range of 350-2500 nm, with a step of 0.5 nm.

3 Results and discussion

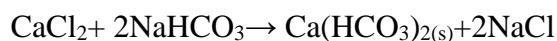
The main goal of this work was to obtain calcite (the most stable polymorph of calcium carbonate) by precipitation synthesis and also by dip-coating directly into a glass substrate.

For the precipitation synthesis several parameters were tested as already mentioned in the material and methods section. In the following section, the obtained results are presented and discussed.

3.1 Synthesis of CaCO₃ by precipitation

The synthesis of calcium carbonate polymorphs was attempted by varying different process parameters that may influence the growth and the crystal structure.

The calcium carbonate is obtained from the reaction of the CaCl₂ (calcium chloride) and NaHCO₃ (sodium bicarbonate) precursors according to the main reaction expected:



(Ethylene glycol)



The above reaction leads to the formation of Ca(HCO₃)₂ (calcium bicarbonate) and NaCl (sodium chloride). Therefore, depending on consumption or not of the all carbonate in the source, the NaCl will be a product of reaction and present in all samples. Knowing that, and as the primary goal is to understand how the process parameters affect the formation of the different CaCO₃ polymorphs, to help this analysis in the following study the NaCl was not removed.

Due to a high number of samples produced and limited access to SEM facilities most of the results obtained are related to the observation of samples in an optical microscope, although it is known that the best type of characterization in order to precisely evaluate the formation of CaCO₃ in any of their polymorphs (calcite, vaterite....) would be EDS and SEM, XRD and also Raman mapping. Nevertheless, as this work consisted in a preliminary study to mimic the natural formation of nacre, we were able to perform an overall screening of the possible synthesis conditions and found out routes to progress in further studies.

3.2 Influence of solution's temperature, magnetic stirring speed and reaction time

The tables of annex 2 show images obtained in the microscope for the different conditions studied. Table A2. 1 shows the images obtained along the time of reaction and two synthesis temperatures 40°C and 75°C for 400rpm stirring. Table A2. 2 shows the evolution of eleven samples when stirring varies to 800rpm. Table A2. 3 the images for synthesis performed without stirring and Table A2. 4 shows the influence of the ultra sounds bath in five samples. A small drop of solution was extracted from the solution recipient, placed in an observation glass and dried in an oven at 70°C prior observation in the microscope. All the images have the same scale to allow a better comparison between them.

From the results some conclusions were taken. First, the time and magnetic stirring speed plays a great role on the formation of crystals, although we think that the bigger crystals are due to NaCl formed, the time in solution promotes the growth of crystals and the speed seems to decrease their size. Therefore, it was performed a new set of four samples without magnetic stirring and lower temperature.

Low temperatures contribute to the formation of smaller crystals; the non-magnetic stirring allows the formation of larger crystals. This was also observed by other authors. Schuler and Tremel said that particles synthesized by microwave heating without magnetic stirring are significantly larger (up to 150 nm) and is mainly calcite; when they increased the temperature the medium size of the particles increased too.[26]

Yu-Bin Hu et al. reported that at near-freezing temperature, precipitation of metastable forms of calcium carbonate from solution is favored (ikaite or vaterite).[51]

3.3 Structural and morphologic analysis

From the all samples produced and due to constrains on access of SEM, Raman and XRD, as mentioned already we try to understand the influence of magnetic stir speed by analysis of samples made with a synthesis time of 60min at 40°C. The influence of temperature was analyzed in samples made at 400rpm and 60min at 40°C and 75°C. The influence of reaction time was observed by comparing results of samples performed at 40°C, 400rpm and 5min, 30 min, 60 min and 24h.

3.3.1 Influence of magnetic stirring

In Figure 6 is shown the SEM images and the optical microscopy images of samples produced at 400 and 800 rpm magnetic stirring at 60 min reaction and temperature 40°C. The Figure 7 a) shows the micro-Raman spectra and Figure 7 b) the XRD pattern of the same samples.

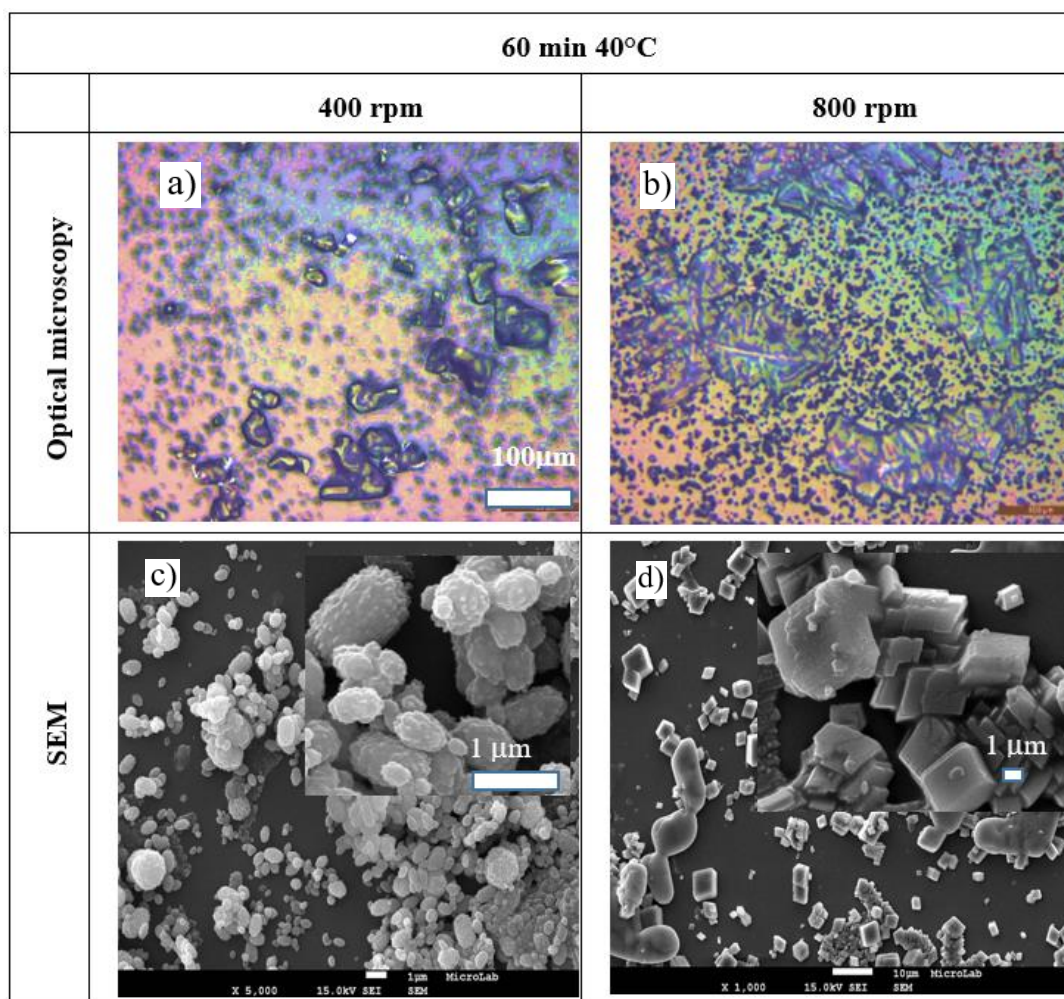


Figure 6 - Images of SEM and optical microscopy for samples synthesized during 60 minutes at 40°C at 400 rpm and 800rpm magnetic stir. a) Optical microscopy of crystals at 400 rpm. b) Optical microscopy of crystals at 800 rpm. c) SEM image of crystals at 400 rpm. d) SEM image of crystals at 800 rpm.

In the optical microscope in Figure 6 a) it is possible to see the bigger crystals of NaCl (halite) and the small dark particles are vaterite agglomerates. In the Figure 6 b) it is possible to see longer halite crystals and a higher concentration of calcite crystals.

The SEM images confirm the difference in the structure of CaCO₃ when magnetic stir changes from 400rpm to 800rpm. Cubic particles are observed for 800rpm while elongated spherulitic particles formed by small crystallites are seen in SEM images when stirring is 400rpm. These structures are typical for calcite and vaterite, respectively.[52][53]

In order to confirm this structure Raman and XRD analysis were performed in the same samples and the results are shown in Figure 7 a) and b) respectively.

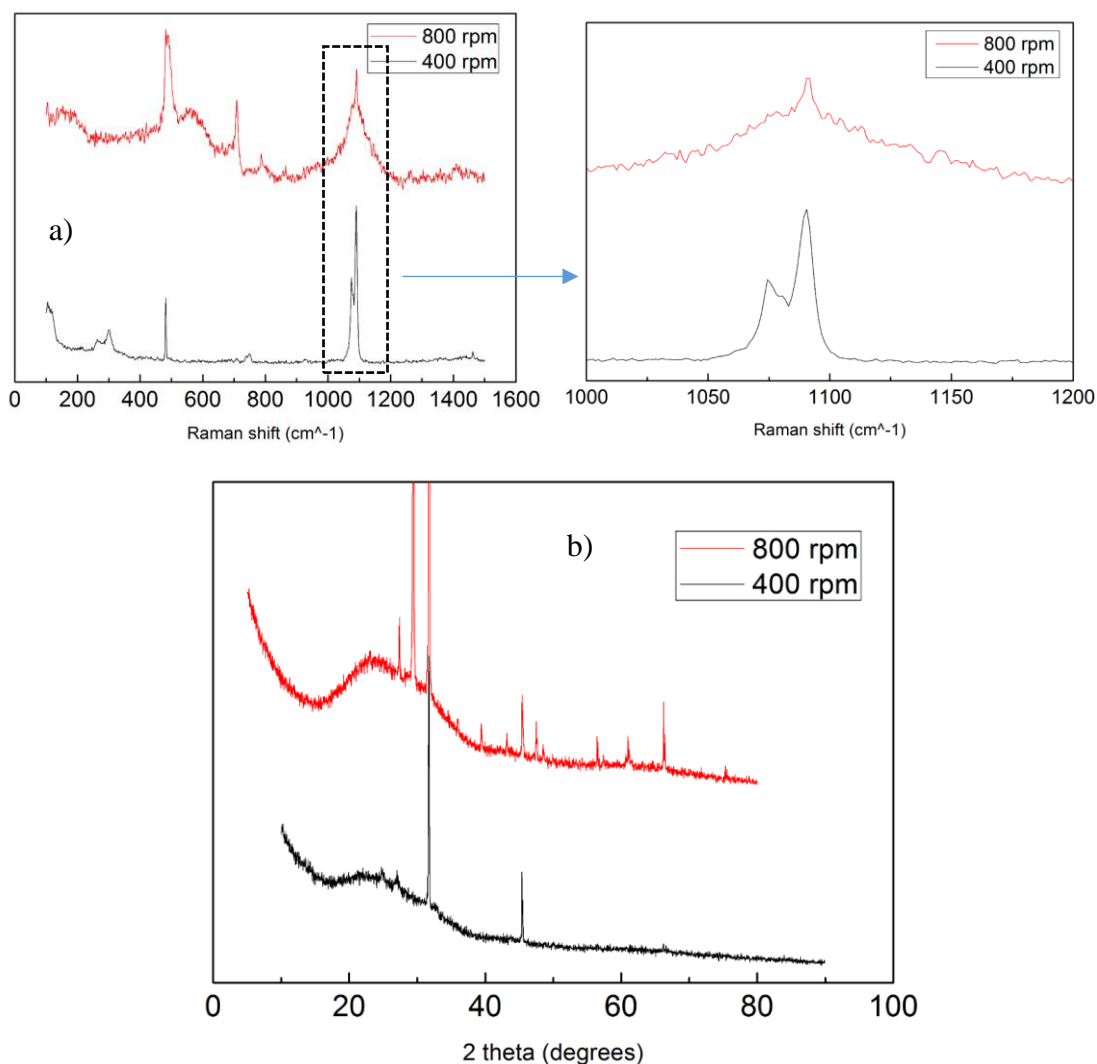


Figure 7- a) – Micro Raman Spectra of samples prepared during 60 min and at 40°C with a different magnetic stir speed b) XRD pattern of samples synthesized at 40°C during 60min with a different rotation speed

Figure 7 a) for 400rpm sample shows the characteristic peaks of vaterite[54]. The presence of symmetric stretching mode triplets with the highest peak at 1090 cm⁻¹, followed by the peak at 1074 cm⁻¹ and the lowest peak at 1081 cm⁻¹; and the presence of in-plane bending mode with a 750 cm⁻¹ peak and the lattice modes peaks at 106 cm⁻¹, 263 cm⁻¹ and 302 cm⁻¹.

Figure 7 a) for 800 rpm sample it is displayed the characteristic peaks of mixed calcite and vaterite in a crystalline/amorphous mixture[55]: a broad symmetric stretching mode peak at 1091 cm⁻¹ from vaterite and an in-plane bending mode at 709 cm⁻¹ slightly shifted to lower wavenumbers peak from calcite. The peak at 482 cm⁻¹ present in both samples is possibly due to the solvent used, ethylene glycol, [56] that was not completely removed during sample drying.

The XRD diffractogram of the same samples are shown in Figure 7 b), the sample synthesized with 400rpm of magnetic stir has two highly intense peaks, one at 31.7° and another at 45.4° which are characteristic of NaCl crystal (halite)[57] (JCPDS card number: 05-0628), but the small peaks at 25°, and at 27° represent vaterite[58]. The sample synthesized at 800 rpm of magnetic stir shows the high characteristic peaks from halite at: 31.7° and the small peaks at: 27°; 45.4°; 56°; 66° and at 75° but also shows the calcite peaks[58] at: 29°, 36°, 39°, 47° and at 61°.

With Scherrer equation it is possible to calculate the crystallite size:

$$D = \frac{K\lambda}{\beta \cos(\theta)}$$

Where D is the mean size of crystallites; K is crystallite shape factor, in this case is 0.94 for FWHM of spherical crystals; λ is the X-ray wavelength, in this case: 0.15418 nm; β is the full width at half the maximum (FWHM) in radians of the X-ray diffraction peak; θ is the Bragg's angle.

For the sample prepared at 400 rpm we have $D = 28.11$ nm; and for the sample prepared at 800 rpm we have $D = 77.09$ nm

3.3.2 Influence of temperature in supersaturation conditions

The influence of temperature was further detailed for samples synthesized during 60 min and magnetic stir of 400 rpm, and as shown previously corresponds to major CaCO₃ vaterite structure. The Figure 8 shows the SEM images and the optical microscopy images of samples obtained with two different temperatures 40°C and 75°C. The Figure 9 a) shows the micro-Raman spectra and Figure 9 b) the XRD pattern of the same samples.

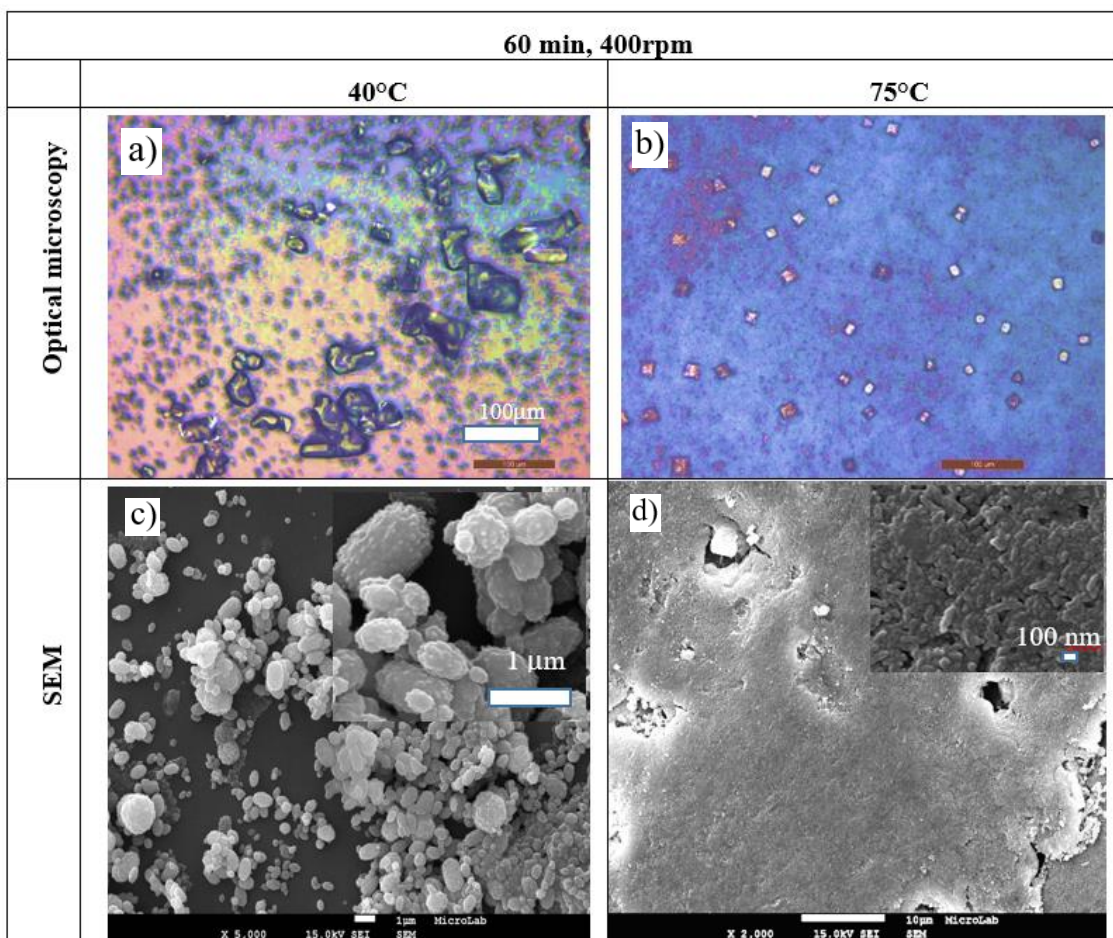
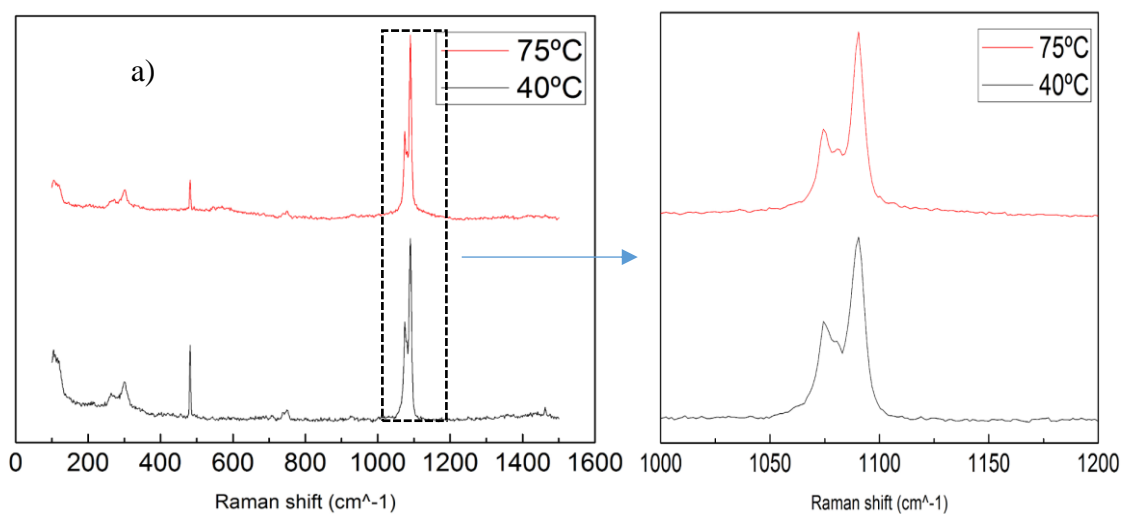


Figure 8 - Images of SEM and optical microscopy for samples synthesized at 40°C and 75°C. a) Optical microscopy of crystals at 40°C; b) Optical microscopy of crystals at 75°C; c) SEM image of crystals at 40°C; d) SEM image of crystals at 75°C.



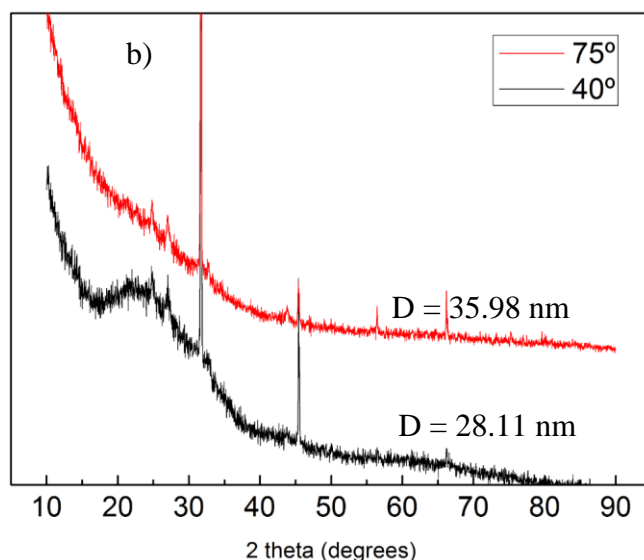


Figure 9 - Samples synthesized during 60 min at 400 rpm with different temperatures: a) Raman spectra; b) XRD pattern.

Figure 8 a) and c) are the same than Figure 6 a) and c). In Figure 8 b) it is possible to see that the NaCl crystals are smaller than in Figure 8 a) but have a more regular cubic shape.

Figure 9 a) compares the Raman spectra of samples synthesized at 40°C and 75°C. The spectrum of sample obtained at 40°C was already presented and identified in Figure 7 a) (400rpm) being identified the respective peaks. Figure 9 b) also shows similar patterns for samples produced with different synthesis temperature. There we see again the main peak of halite at 31.7° and the very small peaks at 45°, 56° and 66°. The peaks at 25°, 27° and 32.8° are from vaterite. Despite the Raman spectra give us the information of vaterite in the sample, in the SEM image of 60 min 75°C 400 rpm we can see unexpectedly what seems to be ACC (amorphous calcium carbonate) [13] because ACC is thermodynamically unstable, and will spontaneously crystallize when suspended in an aqueous solution at ambient temperature.[13]

The XRD data also reveal similar patterns for samples produced at both temperatures and the prevalent diffraction peak is that of halite (NaCl main phase).

3.3.3 Influence of reaction time in supersaturation conditions

The influence of time reaction in the morphology of samples can be observed in Figure 10 by SEM images and the optical microscopy photographs of samples obtained at 400rpm and 40°C. The Figure 11 a) shows the micro-Raman spectra and Figure 11b) the XRD pattern of the same samples.

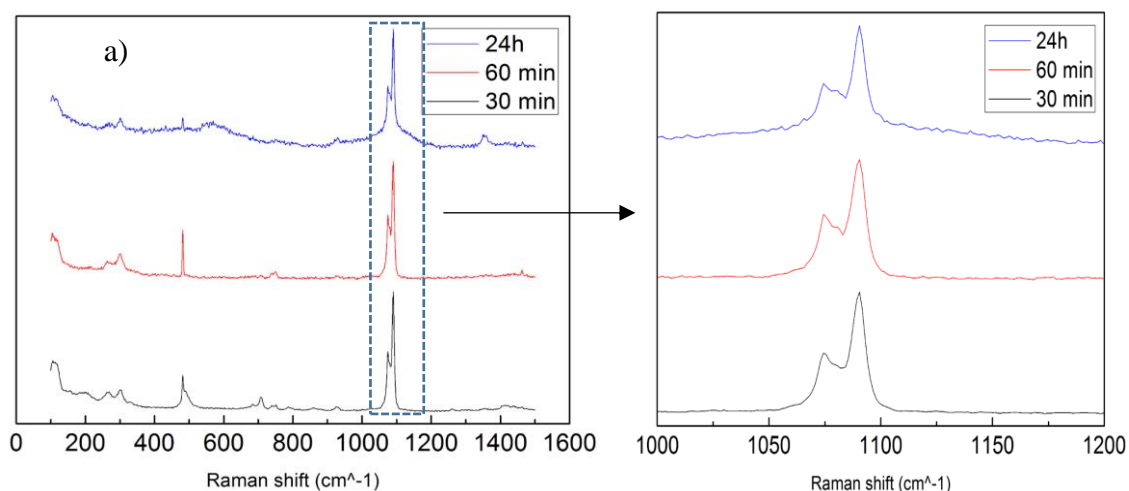
40°C and 400 rpm		
	SEM	Optical microscopy
5 min		
30 min		
60 min		
24h		

Figure 10 - Images of SEM and optical microscopy for samples synthesized at different reaction times: a) SEM image of crystals at 5 minutes reaction time; b) Optical microscope image of crystals at 5 minutes reaction time; c) SEM image of crystals at 30 minutes reaction time; d) Optical microscope image of crystals at 30 minutes reaction time; e) SEM image of crystals at 60 minutes reaction time; f) Optical microscope image of crystals at 60 minutes reaction time; g) SEM image of crystals at 24 hours reaction time; h) Optical microscope image of crystals at 24 hours reaction time.

In the Figure 10 b) it is possible to see halite crystals with a near cubic-shape and the small dark spots are vaterite aggregates. In Figure 10 d) the dark spots with square shape represent the halite crystals and small white spots are a mix between aragonite and vaterite. Figure 10 f) is the same as Figure 8 a). In Figure 10 h) there are not halite crystals present but it is possible to see the small dark spots from vaterite.

Analysing the SEM images above we can see that the reaction time of the solution does not change much the type of polymorph, but the size does change with a longer reaction time. The Raman spectra and XRD patterns shows vaterite as predominate phase unchanged for the time reaction tested. With 30 minute reaction we could observe some aragonite crystals (identified by the needle-like crystals) and one aragonite peak located at 707 cm^{-1} also identified in the Raman spectra, beside the others already identified as being due to vaterite phase. Usually aragonite appears only at higher temperatures and in the presence of Magnesium and Mg^{2+} ions [19]. At 24 hours reaction time the crystal size decrease abruptly becoming very similar to the asteriscus's vaterite which is a constituent of the otolith, a calcium carbonate biomineral present in the fish inner ear [59]

The XRD data shows a high intensity peak of halite (NaCl) at 31.7° in the 3 samples. Although with lower intensity in the 30 minutes' sample the peaks of vaterite are present and located at 25° , 27° , 32.8° and 43.8° ; it is possible to see also one calcite peak at 29.4°



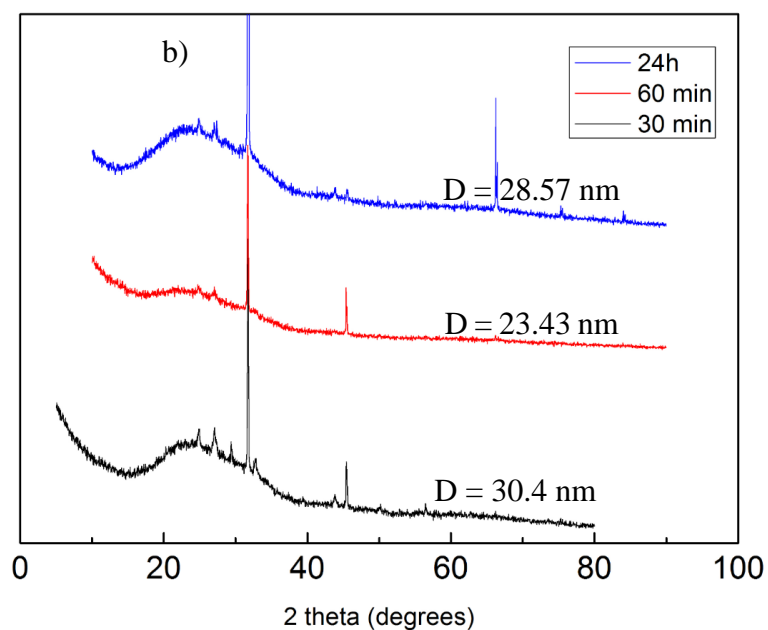


Figure 11 - Samples synthesized at 400 rpm and 40°C at different reaction time: a) Micro Raman spectra; b) XRD pattern.

3.3.4 Influence of $\text{CaCl}_2:\text{NaHCO}_3$ ratio

Although the previous study was performed with the ratio of $\text{CaCl}_2 \cdot \text{H}_2\text{O}:\text{NaHCO}_3$ (1:2) given by the literature [26] we have tried also to vary the ratio of the precursors and find out its influence on the calcium carbonate polymorphs.

In Figure 12 are shown the microscopy and SEM images of obtained samples for the different ratios tested keeping the reaction temperature at 40°C and magnetic stir at 400rpm. Figure 14 shows the Raman Spectra and XRD pattern of the same samples.

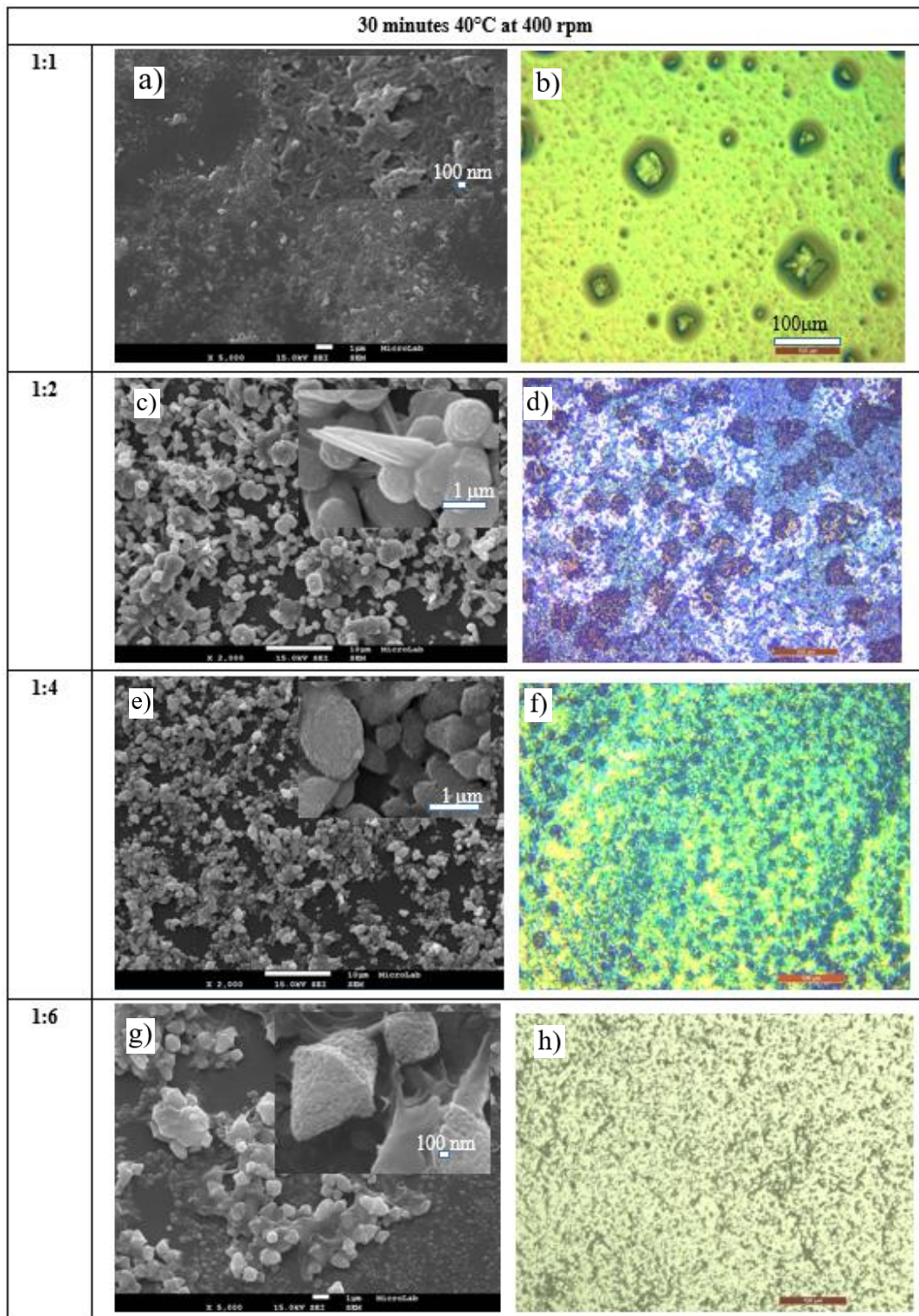


Figure 12 - Microscopy and SEM images of samples synthesized at 40°C during 30 minutes for magnetic stir of 400 rpm varying $\text{CaCl}_2 \cdot 2\text{H}_2\text{O}:\text{NaHCO}_3$ ratios; a) SEM image of (1:1 ratio); b) Optical microscope image of (1:1 ratio); c) SEM image of (1:2 ratio); d) Optical microscope image of (1:2 ratio); e) SEM image of (1:4 ratio); f) Optical microscope image of (1:4 ratio); g) SEM image of (1:6 ratio); h) Optical microscope image of (1:6 ratio).

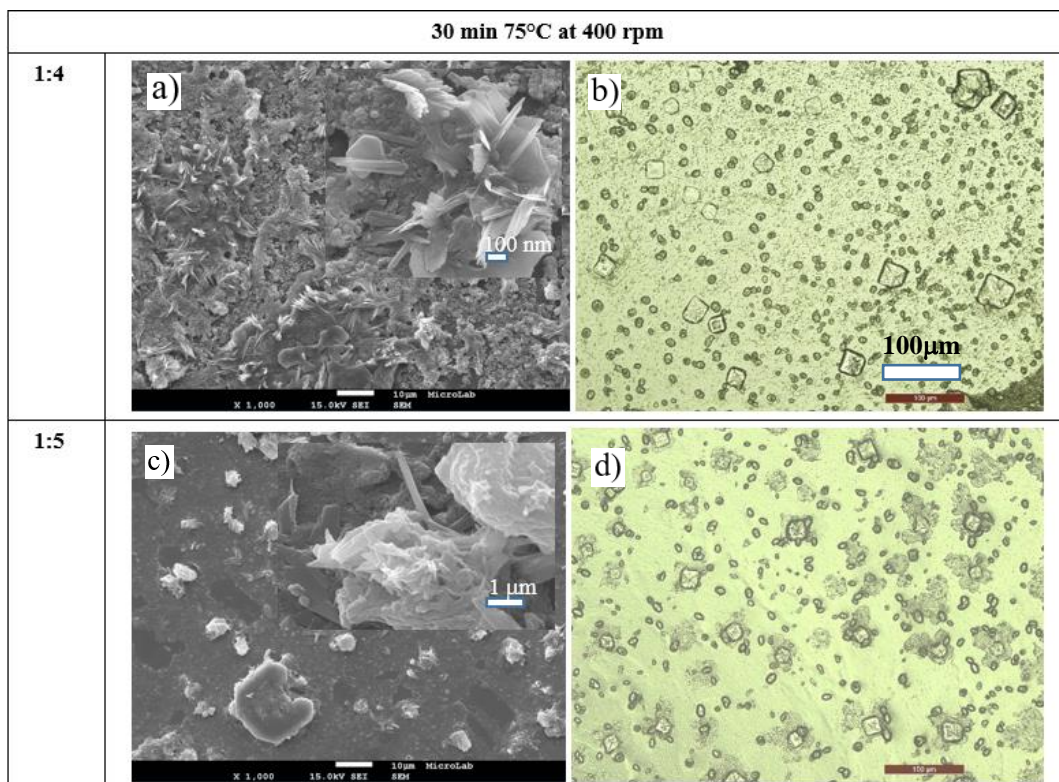


Figure 13 - Microscopy and SEM images of samples synthesized at 75°C during 30 minutes for magnetic stir at 400 rpm varying $\text{CaCl}_2 \cdot 2\text{H}_2\text{O}:\text{NaHCO}_3$ ratios: a) SEM image of (1:4 ratio); b) Optical microscope image of (1:4 ratio); c) SEM image of (1:5 ratio); d) Optical microscope image of (1:5 ratio)

Figure 12 d) has the biggest NaCl crystals compared to the other samples, increasing NaHCO_3 concentration, the NaCl crystals become smaller.

The SEM images of Figure 12 complemented by microscopy images show how the morphology of samples is influenced by the concentration of NaHCO_3 as the one of CaCl_2 is kept constant. A 1:1 ratio the morphology of samples look-like amorphous calcium carbonate (ACC) and this is confirmed in the Raman spectra of Figure 14 a). Increasing the NaHCO_3 amount into the solution (1:4) we get spheres of vaterite with some aragonite. Further increase of NaHCO_3 in the solution (1:6 ratio of $\text{CaCl}_2:\text{NaHCO}_3$) we get enhanced size crystal with an unusual shape (a double-cone like shape). In the Raman spectra of Figure 14 it corresponds to a shift to lower wavenumber of vaterite peaks to unknown peaks position: 1030 cm^{-1} , 1062 cm^{-1} and 1084 cm^{-1} . Those peaks are due to a greater increase of NaHCO_3 (sodium bicarbonate) in the solution. The morphology shown in the SEM images of vaterite forming such a kind of a double spinning top toy shape that to our knowledge was never seen before.

Increasing the temperature with a concentration of NaHCO_3 of 1:4 and 1:5 we got a smooth like structure with plate-like shape characteristic of aragonite as can be seen in the SEM image of the sample (1:4) 30 min 75°C at 400 rpm. The corresponding Raman spectrum shows

one peak of aragonite at 700 cm^{-1} [54]; we can also see similar peaks on sample: 30 min 40°C 400 rpm (1:6); at 1027 cm^{-1} , 1062 cm^{-1} .

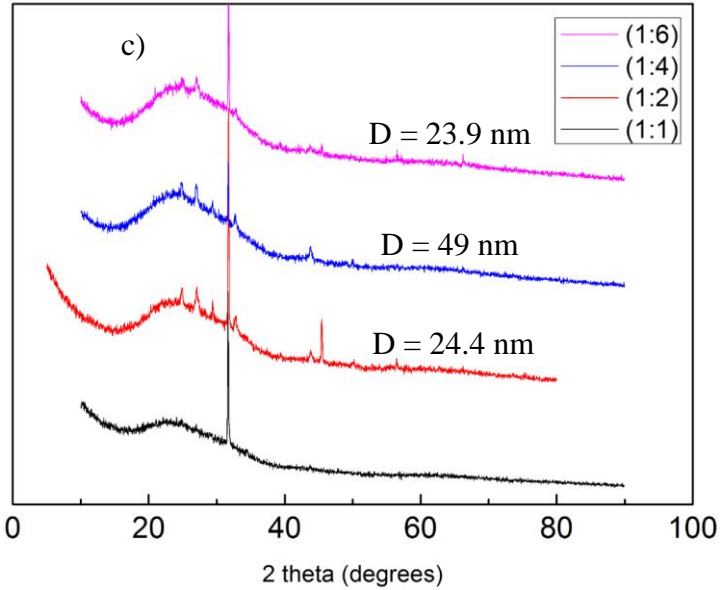
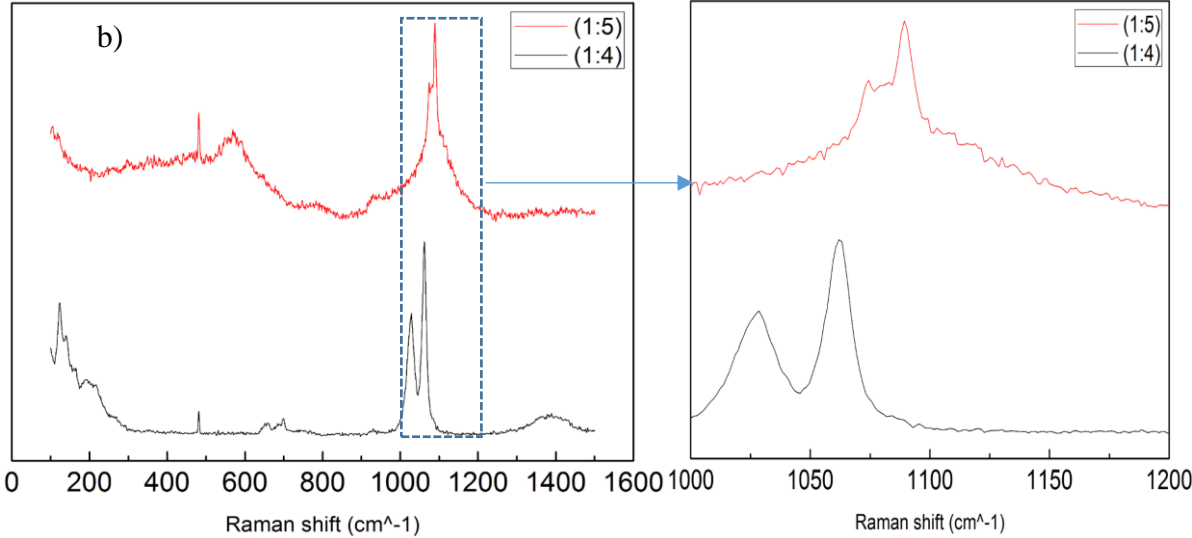
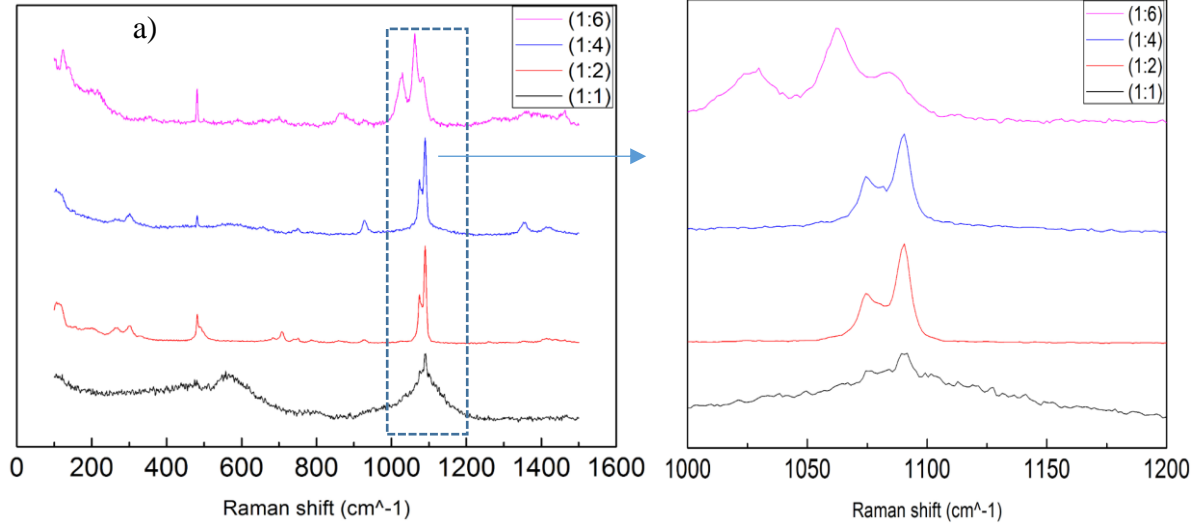
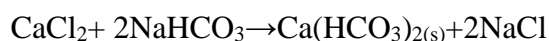


Figure 14 - a) Micro Raman spectra of 4 samples synthesized during 30 minutes at 40°C at 400 RPM with different reagents (CaCl₂*2H₂O/(NaHCO₃)₂) ratios. b) Micro Raman spectra of 2 samples synthesized during 30 minutes at 75°C at 400 rpm with different reagents (CaCl₂*2H₂O/(NaHCO₃)₂) ratios. c) XRD pattern of 4 samples synthesized during 30 minutes at 40°C at 400 RPM with different reagents (CaCl₂*2H₂O/(NaHCO₃)₂) ratios.

For the sample with ratio of 1:1 there are not characteristic peaks from calcium carbonate, so the crystallite size cannot be calculated.

3.4 Purified calcium carbonate powders

The previous study was performed on the samples just as it is synthesized, that is, without any further treatment. Therefore, most of the samples had a high quantity of NaCl which results from the reaction:

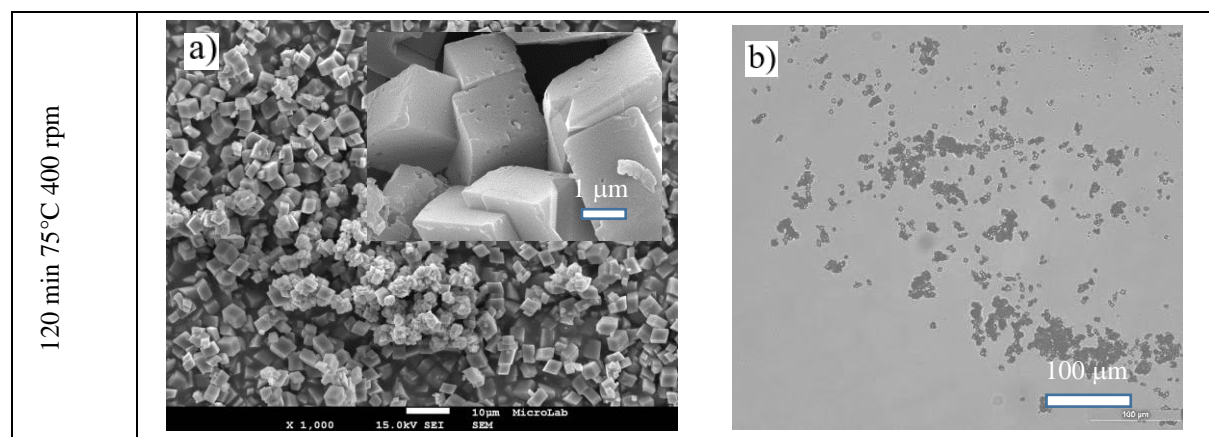


(Ethylene glycol)



Even knowing that NaCl formed is always the same, as the CaCl₂ is the limiting reactant of the above reaction, it can influence the formation of the CaCO₃ polymorphs. Therefore, in some of the obtained samples the reactions' products were washed several times in water and ethanol to eliminate NaCl.

The obtained SEM and microscopy images are shown in Figure 15 for the different synthesis conditions used. The corresponding Raman and XRD spectra are shown in Figure 16 a) and b) respectively



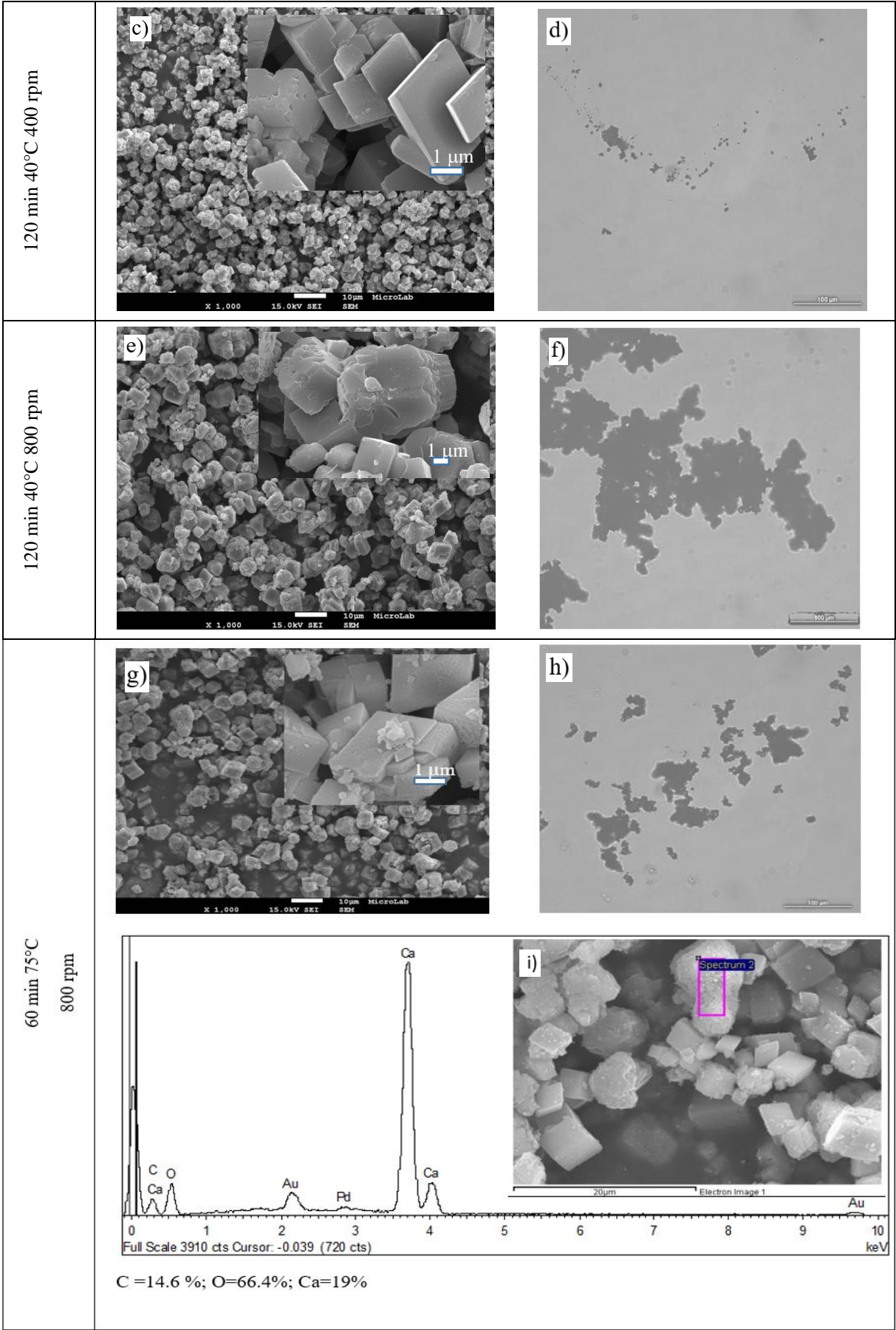
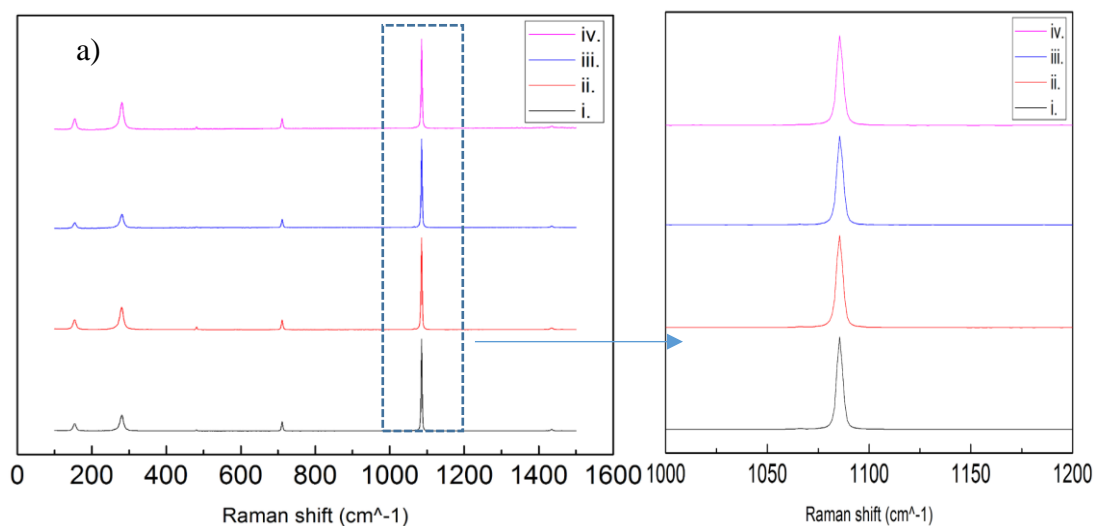


Figure 15 - SEM, microscopy and EDS images of samples washed after preparation: a) SEM image of crystals at 120 minutes 75°C 400 rpm; b) Optical microscope image of crystals at 120 minutes 75°C 400 rpm; c) SEM image of crystals at 120 minutes 40°C 400 rpm; d) Optical microscope image of crystals at 120 minutes 40°C 400 rpm; e) SEM image of crystals at 120 minutes 40°C 800 rpm; f) Optical microscope image of crystals at 120 minutes 40°C 800 rpm; g) SEM image of crystals at 60 minutes 75°C 800 rpm; h) Optical microscope image of crystals at 60 minutes 75°C 800 rpm; i) EDS spectrum of the sample at 60 minutes 75°C 800 rpm.

Analyzing the SEM images in Figure 15 and Raman peaks, the obtained powder samples are all made of calcite. This is confirmed by the 1085, 711, 280 and 155 cm^{-1} Raman peaks characteristic of calcite [54]. XRD patterns also show the characteristic diffraction peaks of pure calcite at: 29.5°; 36°; 39.5°; 43°; 47.5° and 48.5°[58] The samples prepared rested for 1 month, being extracted 1 mL of solution, washed and dried as stated in the procedure; and as expected vaterite turned into calcite as mentioned by Rodriguez-Blanco et-al[13]. The state for similar reagents and with lower reaction temperature in a Teflon reaction cell, that after 1 hour vaterite crystals begin to transform into calcite crystals and after 20 hours all the vaterite turned into calcite. They also showed that increasing the temperature vaterite turns into calcite faster.

In our experiments, initial parameters do not seem to modify much the final result, just with increased rotation speed it is possible to note some small crystals aggregated to bigger ones.



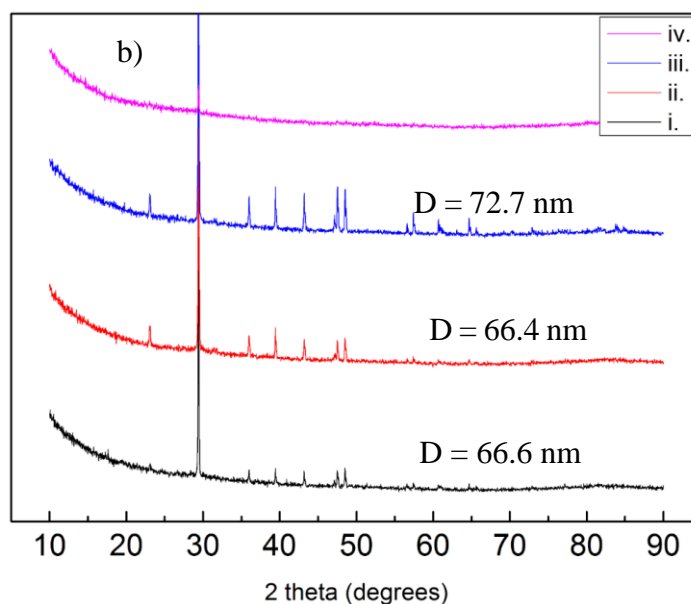


Figure 16- a) Micro Raman spectra and b) XRD pattern of samples washed after synthesis: i. 120 min 75° and 400rpm; ii. 120 min 40° and 400rpm; iii. 120 min 40° and 800rpm and; iv. 60 min, 75° and 800rpm

3.5 Synthesis of CaCO₃ films by Dip-Coating

The dip coating was tested with the goal of obtaining directly the calcite films onto a glass substrate. Many parameters of the dip coater can be changed and may influence the final properties of the films. In the following are shown the results obtained for the selected preparation conditions.

3.5.1 Influence of the number of cycles and dip velocity

The influence of dip-coating number of cycles for different conditions: velocity and time of dip (time duration in which the samples was immersed in the calcium carbonate solution) on the absorbance at 1500 nm wavelength are shown in Figure 17. As the absorbance is proportional to the film thickness, we can say that immersing the glass substrate at higher velocity leads to the formation of thicker films. This can be seen by comparing data of 500 μ m/s and 5mm/s and 3 min dip where the absorbance has a great enhancement for 10 cycles. Keeping the dip velocity ten times lower and increasing the dip time we do not see any remarkable influence, at least for 10 cycles.

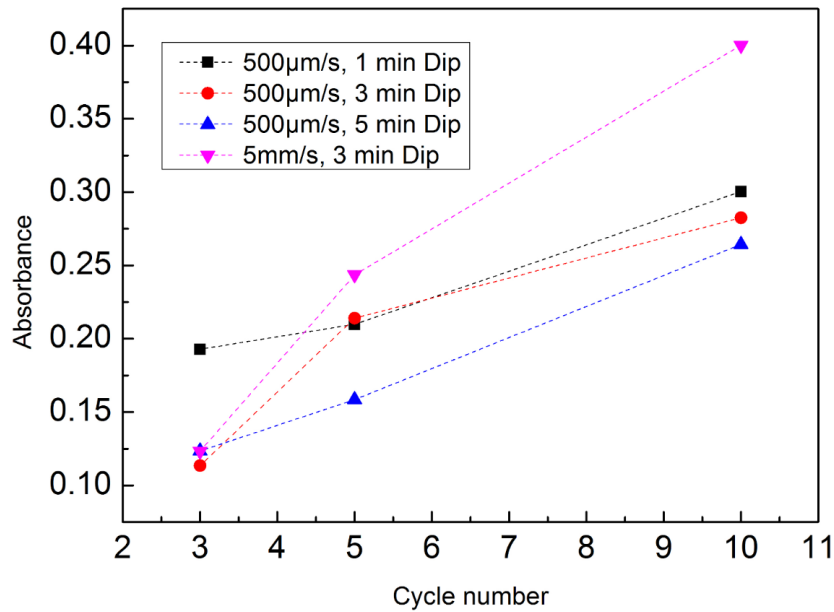


Figure 17 - Absorbance at 1500 nm versus number of cycles varying the dip time keeping constant T=40°C and 3 min Dry.

The complete study of absorbance spectra for the different coating conditions are shown in Table A3. 1 of annex 3.

3.5.2 Dip-coating with organic compounds (PVP)

In order to mimic nacre and since it is formed with organic compounds, and based on the literature[60] we have tried different conditions for dip-coating with calcium carbonate and organic compounds, PVP. Two different approaches were tested: dip-cycles of glass being immersed sequentially in CaCl₂ followed by NaHCO₃ and at last PVP, being the cycle repeated different times and the absorbance spectra of samples acquired in the spectrophotometer. The absorbance at 500 nm was plotted as a function of number of cycles and shown in Figure 18. The absorbance was compared at 500 nm due to a higher difference in the absorption spectra, as can be seen in the Figure 19. The complete study on the influence of dip-coating parameters studied on the absorbance spectra and the corresponding microscopy images are in the Table A3. 1 of annex 3.

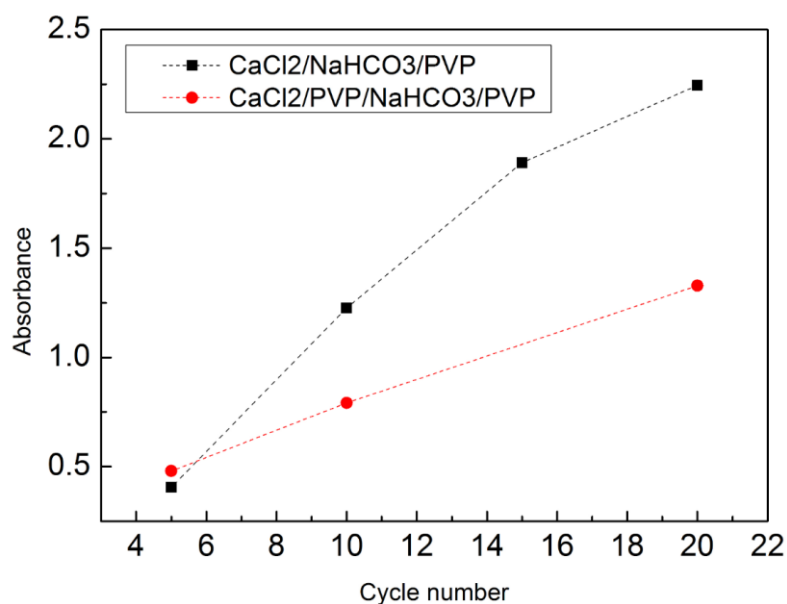


Figure 18 - Absorbance as a function of the number of cycles at 500 nm for different sequences; cycle of 2min dip in the PVP, and 3 min dry for a dip speed 5mm/s, ambient temperature of 27°C and 10 seconds of dip time in the inorganic reagents.

Clearly is shown a linear increase of the absorbance at 500 nm with the number of cycles for both dip-conditions, however the films growth faster when first is formed the CaCO₃ with the sequence of dip in CaCl₂ and NaHCO₃ and then immersed in PVP than when it is immersed in PVP in between. Although the PVP layer formed in a single dip is thinner it seems to be thicker enough to cover some CaCl₂ firstly adsorbed in the glass surface and prevents its reaction with NaHCO₃ in the subsequent dip.

Other sequences were also tried and the absorption and reflectance spectra of samples produced with 10 dip-coating cycles are shown in Figure 19 a) and b) respectively. Besides the absorbance spectra of CaCl₂/NaHCO₃/PVP and CaCl₂/PVP/NaHCO₃/PVP corresponding to the Figure 19 was also tested CaCO₃/PVP and CaCl₂/sea water/PVP. The absorption spectra reveal that samples are absorbing in the visible range while in the infrared region (above 1000nm) are highly transparent-low absorption probably due to a modification in the structure of the samples that should be further investigated by SEM.

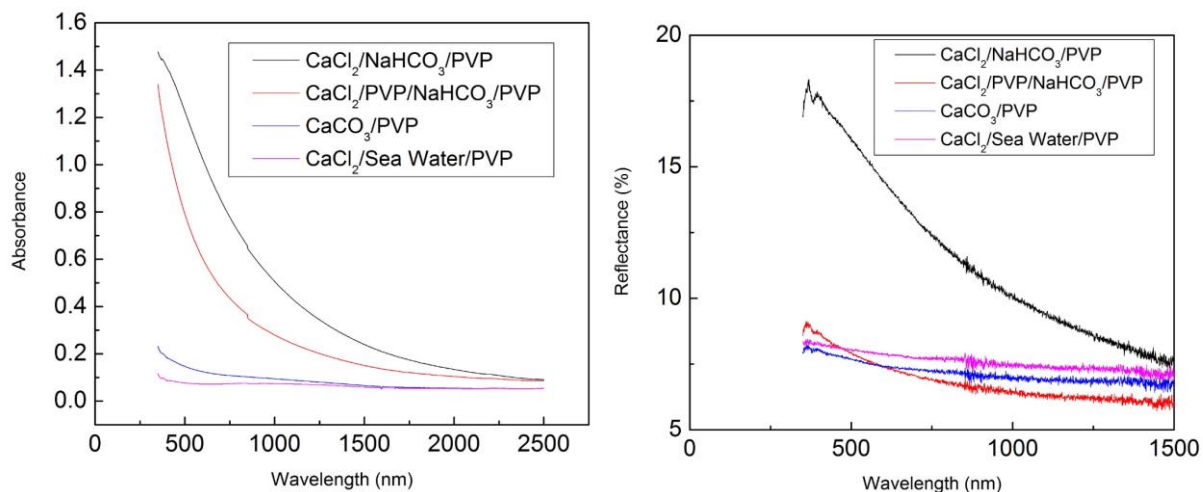


Figure 19 - a) Absorbance and b) reflectance as a function of the wavelength for different sequences of cups at 10 cycles; cycle of 2min dip in the organic cup, and 3 min dry for a dip speed 5mm/s, ambient temperature of 27°C and 10 seconds of dip time in the inorganic reagents.

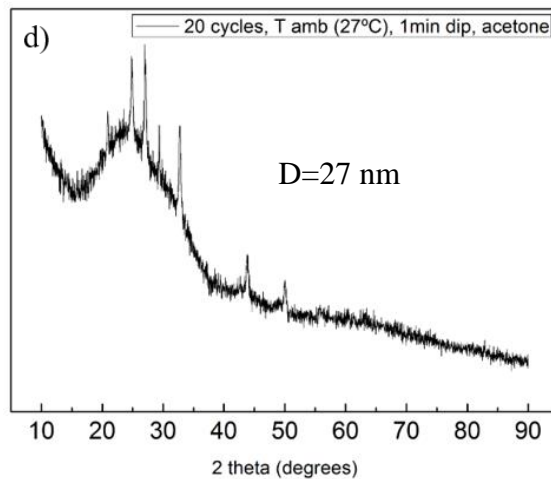
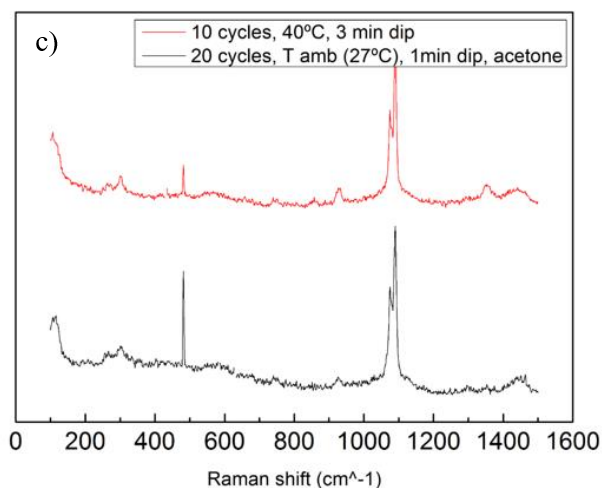
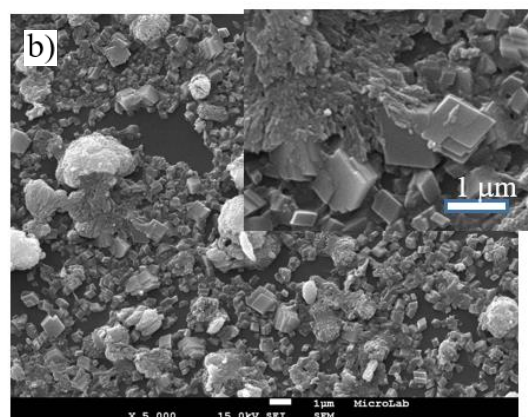
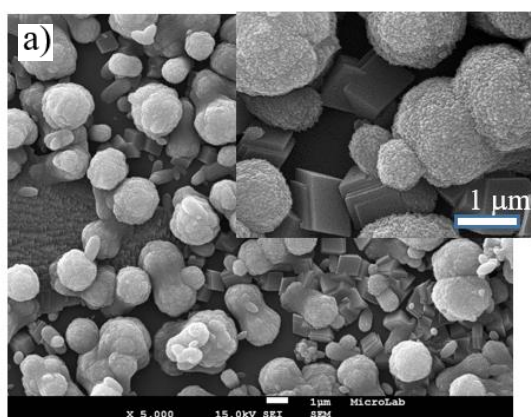


Figure 20 - a) and b) SEM images of the dip coated samples respectively for 20 cycles, T amb(27°C), 1 min dip, acetone and 10 cycles, 40°C, 3 min dip; c) Raman spectra of dip-coated samples at 5 mm/s and 3 min dry time with different number of cycles, different temperature, different dip and with/without in-between cup, d) XRD pattern of sample dip- coated at ambient temperature and at 5 mm/s with cup of acetone dipped during 2 secs in-between the inorganic cups

The Raman spectra of two dip-coated samples we can see the characteristic peaks from vaterite [54] the v1 (symmetric stretching mode) triplets with the highest peak at 1090 cm^{-1} , followed by the peak at 1075 cm^{-1} and the lowest intensity peak at 1081 cm^{-1} ; the v4 (in-plane bending mode) with a 751 cm^{-1} peak and the (lattice modes) peaks at 106 cm^{-1} , 265 cm^{-1} and 301 cm^{-1} . In the (black lower graph) we can see that the peak at 482 cm^{-1} has a higher intensity than the peak in red upper graph comparatively with the v1 peaks, this means there is more concentration of ethylene glycol when acetone is in the solution. The characteristic peaks of XRD from vaterite at: 25° , 27° , 33° , 44° and 50° and the highest peak of calcite at 29° .

4 Conclusions and future perspectives

One of the goals of this thesis was to obtain pure CaCO_3 by chemical reaction. Several parameters of the reaction were modified in order to understand their influence in the formation of CaCO_3 polymorphs. The changed parameters of the reaction were: temperature, time, stirring speed, different concentration of reagents and influence of the medium (oil bath or ultrasounds). The reactants were CaCl_2 (calcium chloride) and NaHCO_3 (sodium bicarbonate) and the solvent was ethylene glycol ($\text{C}_2\text{H}_6\text{O}_2$).

From this study a generic conclusion based on the observation of samples in microscope was taken: the time and magnetic stirring speed plays a great role on the formation of crystals, the time in solution promotes de growth of crystals and the stirring speed seems to contribute to decrease the size of the formed crystals. Higher temperature contributed to the formation of higher crystals and the absence of magnetic stirring lead to the formation of larger crystals.

A more detailed analysis based on the SEM, Raman, XRD e EDS analysis lead to the following conclusions:

- The variation of magnetic stirring from 400rpm to 800rpm induces a change of CaCO_3 in the form of vaterite to calcite.

This was confirmed by the morphology of crystals formed, vaterite contains very small crystals that are aggregated to form elongated structures. Raman and XRD also confirm the existence of the vaterite finger-print peaks. A high intense doublet-peak at 1090 and 1074cm^{-1} in Raman spectra, while by XRD the peaks of vaterite at 25° and 27° are present. The calcite was identified by its typical morphology in SEM images, the cubic shape of crystals with a wide dispersion of sizes, from nanometers to dozen of micrometers and confirmed in XRD pattern with the main intense peak at 29° related to (104) diffraction planes.

- The temperature and reaction time has no influence on CaCO_3 structure, although it seemed to enhance the growth of crystals.

In fact, the SEM images show more compact structure formed by collate nanometric crystals when the synthesis temperature is 75°C instead 40°C . Raman spectra and XRD patterns are very similar for samples synthesized at these temperatures. While for the reaction time the quantity of vaterite crystals are significantly higher for the same quantity of solution sampled.

- The variation of $\text{CaCl}_2 \cdot 2\text{H}_2\text{O}:\text{NaHCO}_3$ ratios for samples synthesized at 40°C and 75°C for magnetic stir of 400rpm plays an important role on the CaCO_3 structure.

Although the CaCO_3 crystals are mainly formed by vaterite, the crystals aggregation strongly depends on the ratio used. Crystals formed with 1:1 ratio are nanometric with uniform aggregation forming very small needle-like structures involved by amorphous calcium carbonate. Spherical aggregation is the prevalent crystals structure for the samples synthesised

at 1:2 ratios, some aragonite is also formed at this ratio. For the ratio 1:4 the aggregation forms a double-cone like shape, very unusual, the same is obtained for 1:6 ratios, in these also amorphous calcium carbonate was observed. The enhancement of temperature to 75°C for the 1:4 and 1:5 ratios leads to the formation of aragonite plate-like structure.

All the above conclusions were taken from the study performed without purification of samples and so the NaCl, as a product of reaction, is always present.

The purification of crystals was performed by washing the obtained solutions in water and ethanol and then centrifugation, being obtained pure calcite.

The second goal of this work was to explore dip-coating technique as an attempt to produce nacre alternating between an organic and inorganic solution. Several parameters varied such as temperature, dip and dry time, with/without in-between cup, number of cycles, dipping speed.

We conclude that for the dipping speed studied 500 μ m/s and 5mm/s the absorbance is higher for later for the same number of cycles. When alternating the reaction of CaCl₂ and NaHCO₃ the growth of films increases, although it is more remarkable for the sequence CaCl₂/NaHCO₃/PVP than for CaCl₂/PVP/NaHCO₃/PVP. The obtained films are formed by a mixture of vaterite and calcite.

From this work we can conclude that it is possible to produce calcium carbonate and its polymorphs in simple ways like the classical precipitation method and the new dip-coating method. The conditions of obtaining, by chemical reaction, vaterite, calcite or aragonite were identified. By dip-coating technique we got a mixture of the reactants of calcium carbonate with an organic solution of PVP and obtained an organic/inorganic complex nacre-like structure.

Overall, a background study was performed that could be explore in further works. Other variations of the parameters in the solution and in the dip-coating can be explored like the further increase of the temperature and the addition of Mg in the solution to obtain aragonite and produce iridescent nacre instead of the lackluster compound obtained.[12]

Functionalize the organic matrix with some functional groups like carboxyl (-COOH) or hydroxyl (-OH) to help the mineralization.[41][61]

References

- [1] S. Mann, *Biom mineralization*. Oxford Chemistry Masters, 2001.
- [2] Y. Guo, F. Wang, J. Zhang, and L. Yang, “Biomimetic synthesis of calcium carbonate with different morphologies under the direction of different amino acids” pp. 2407–2415, 2013.
- [3] P. Somasundaran and G. . Agar, “The zero point of charge of calcite” *J. Colloid Interface Sci.*, vol. 24, no. 4, pp. 433–440, 1967.
- [4] F. Lippmann, *Sedimentary Carbonate Minerals*, vol. 6. Springer, 1973.
- [5] J. Rieger, T. Frechen, G. Cox, C. Schmidt, and J. Thieme, “Precursor structures in the crystallization/precipitation processes of CaCO₃ and control of particle formation by polyelectrolytes” *Faraday Discuss.*, no. 136, pp. 265–277, 2007.
- [6] L. Gower, “Biomimetic model systems for investigating the amorphous precursor pathway and its role in biomineralization,” *Chem. Rev.*, vol. 108, pp. 4551–4627 2008.
- [7] D. Gebauer, “Proto-Calcite and Proto-Vaterite in Amorphous Calcium Carbonates” *Angew. Chemie-International Ed.*, vol. 49, no. 47, pp. 8889–8891, 2010.
- [8] H. Deng, X. C. Shen, X. M. Wang, and C. Du, “Calcium carbonate crystallization controlled by functional groups : A mini-review” *Front. Mater. Sci.*, vol. 7, no. 1, pp. 62–68, 2013.
- [9] “https://www.healingcrystals.com/Aragonite_-_Aragonite_Clusters__Morocco_.html.” . accessed in 2016-10-07

- [10] “http://scitec.uniurb.it/dipartimenti/digeoteca/collezionefranchin/campioni_per_classe.php?classe=Carbonati%20e%20Nitrati.” . accessed in 2016-10-07
- [11] “<http://geology.com/minerals/calcite.shtml>.” . accessed in 2016-10-07
- [12] M. Pérez-estébanez, Š. Radek, M. Pérez-estébanez, A. Viani, Š. Petr, and P. Mácová, “Characterization of vaterite synthesized at various temperatures and stirring velocities without use of additives” *Powder Technol.*, vol. 284, no. November, pp. 265–271, 2015.
- [13] J. D. R. Blanco, S. Shawa, and L. G. Benninga, “The kinetics and mechanisms of amorphous calcium carbonate (ACC) crystallization to calcite, viavaterite.” *Nanoscale*, vol. 3, pp. 265–271, 2011.
- [14] J. Carmona, J. Gómez-Morales, and R. R. Clemente, “Rhombohedral-scalenohedral calcite transition produced by adjusting the solution electrical conductivity in the system Ca(OH)(2)-CO2-H2O” *J. Colloid Interface Sci.*, vol. 261, pp. 434–440, 2003.
- [15] S. R. Dickinson, G. E. Henderson, and K. M. McGrath, “Controlling the kinetic versus thermodynamic crystallisation of calcium carbonate” *J. Cryst. Growth*, vol. 244, no. 3–4, pp. 369–378, 2002.
- [16] N. Spanos and P. Koutsoukos, “Kinetics of Precipitation of Calcium Carbonate in Alkaline pH at Constant Supersaturation. Spontaneous and Seeded Growth” *J. Phys. Chem. B*, vol. 102, no. 34, pp. 6679–6684, 1998.
- [17] G. Hadiko, Y. S. Han, M. Fuji, and M. Takahashi, “Synthesis of hollow calcium carbonate particles by the bubble templating method” *Mater. Lett.*, vol. 59, no. 19–20, pp. 2519–2522, 2005.
- [18] Y. S. Han, G. Hadiko, M. Fuji, and M. Takahashi, “Influence of initial CaCl2 concentration on the phase and morphology of CaCO3 prepared by carbonation” *J. Mater. Sci.*, vol. 41, no. 14, pp. 4663–4667, 2006.
- [19] C. Y. Tai and F.-B. Chen, “Polymorphism of CaCO3, precipitated in a constant-composition environment” *AIChE J.*, vol. 44, no. 8, pp. 1790–1798, 1998.

- [20] R. Dongni, G. Yonghua, and F. Qingling, “Comparative study on nano-mechanics and thermodynamics of fish otoliths.” *Mat. Sci. Eng. C-Mater*, vol. 33, pp. 9–14, 2013.
- [21] N.A. Palchik and T. N. Moroz, “Polymorph modifications of calcium carbonate in gallstones” *J. Cryst. Growth*, vol. 283, no. 3–4, pp. 450–456, 2005.
- [22] J. Renkel, S. Hobe, M. Susewind, and D. E. Jacob, “Designed peptides for biomineral polymorph recognition : a case study for calcium carbonate” *J. Mater. Chem. B*, vol. 3, pp. 3511–3518, 2014.
- [23] L. Qiao, Q. L. Feng, and Z. Li, “Special Vaterite Found in Freshwater Lackluster Pearls” *Cryst. Growth Des.*, vol. 7, no. 2, pp. 275–279, 2007.
- [24] R. G. Jones and W. L. Davis, “Calcium-containing lysosomes in the outer mantle epithelial cells of *Amblema*, a fresh-water mollusc” *Anat. Rec.*, vol. 203, no. 3, pp. 337–343, 1982.
- [25] D. Ren, O. Albert, W. Muller, and Q. L. Feng, “Primary cell culture of fresh water *Hyriopsis cumingii* mantle/pearl sac tissues and its effect on calcium carbonate mineralization” *Cryst. Growth Des.*, vol. 14, no. 3, pp. 1149–1157, 2014.
- [26] T. Schuler and W. Tremel, “Versatile wet-chemical synthesis of non-agglomerated CaCO₃ vaterite nanoparticles” *Chem. Commun.*, vol. 47, pp. 5208–5210, 2011.
- [27] Z. Li, T. Wen, Y. Su, X. Wei, C. He, and D. Wang, “Hollow hydroxyapatite spheres fabrication with three-dimensional hydrogel template” *CrystEngComm*, vol. 16, pp. 4202–4209, 2014.
- [28] Y. Jia, T. Luo, X.-Y. Yu, J.-H. Liu, and X.-J. Huang, “Surfactant-free preparation of nickel carbonate hydroxide in aqueous solution and its toxic ion-exchange properties” *New J. Chem.*, vol. 37, pp. 534–539, 2013.
- [29] Y. Guo, W. Jia, H. Li, W. Shi, J. Zhang, and J. Fenga, “Facile green synthesis of calcium carbonate/folate porous hollow spheres for the targeted pH-responsive release of anticancer drugs” *J. Mater. Chem. B*, no. 4, pp. 5650–5653, 2016.

- [30] H. Gleiter, “Nanostructured materials: basic concepts and microstructure” *Acta Mater.*, vol. 48, no. 1, pp. 1–29, 2000.
- [31] G. E, S. WW, U. HS, H. J, N. F, M. B, and Z. A, “Homoepitaxial meso- and microscale crystal co-orientation and organic matrix network structure in *Mytilus edulis* nacre and calcite.” *Acta Biomater.*, vol. 9, no. 12, pp. 9492–9502, 2013.
- [32] “<http://nature.berkeley.edu/classes/eps2//wisc/oLect17.html>.” . accessed in 2016-10-07
- [33] “<http://www.nautilusdivingbali.com/about-nautilus>.” . accessed in 2016-10-07
- [34] S. Hamza, N. Slimane, Z. Azarib, and G. Pluvinageb, “Structural and mechanical properties of the coral and nacre and the potentiality of their use as bone substitutes” *Appl. Surf. Sci.*, vol. 264, pp. 485–491, 2013.
- [35] N. H. Munro and K. M. McGrath, “How important is polyelectrolyte complex formation in biomimetic mineralisation? Manipulation via alcohol addition” *Dalt. Trans.*, vol. 42, no. 23, pp. 8259–8269, 2013.
- [36] H. Xu, K. Huang, Q. Gao, Z. Gao, and X. Han, “A study on the prevention and treatment of myopia with nacre on chicks.” *Pharmacol Res.*, vol. 44, no. 1, pp. 1–6, 2001.
- [37] M. Lamghari, M. . Almeida, S. Berland, H. Huet, A. Laurent, C. Milet, and E. Lopez, “Stimulation of bone marrow cells and bone formation by nacre: in vivo and in vitro studies” *Bone*, vol. 25, no. 2, p. 91s–94s, 1999.
- [38] M. Lamghari, S. Berland, A. Laurent, H. Huet, and E. Lopez, “Bone reactions to nacre injected percutaneously into the vertebrae of sheep” *Biomaterials*, vol. 22, no. 6, pp. 555–562, 2001.
- [39] E. Lopez, A. Le Faou, S. Borzeix, and S. Berland, “Stimulation of rat cutaneous fibroblasts and their synthetic activity by implants of powdered nacre (mother of pearl)” *Tissue Cell*, vol. 32, no. 1, pp. 95–101, 2000.

- [40] E. Munch, M. Launey, D. Alsem, E. Saiz, A. Tomsia, and R. Ritchie, “Tough, bio-inspired hybrid materials” *Science*, vol. 322, no. 5907, pp. 1516–1520, 2008.
- [41] A. Finnemore, P. Cunha, T. Shean, S. Vignolini, S. Guldin, M. Oyen, and U. Steiner, “Biomimetic layer-by-layer assembly of artificial nacre” *Nat. Commun.*, vol. 3, no. 966, 2012.
- [42] J. E. Parker, S. P. Thompson, A. R. Lennie, J. Pottera, and C. C. Tang, “A study of the aragonite-calcite transformation using Raman spectroscopy, synchrotron powder diffraction and scanning electron microscopy” *CrystEngComm*, vol. 12, pp. 1590–1599, 2010.
- [43] D. Gebauer, A. Völkel, and H. Cölfen, “Stable prenucleation calcium carbonate clusters” *Science.*, vol. 322, no. 5909, pp. 1819–1822, 2008.
- [44] E. S. Tjandra, R. A. Boulos, P. C. Duncanc, and C. L. Raston, “Unfastening pearl nacre nanostructures under shear” *CrystEngComm*, vol. 15, pp. 6896–6900, 2013.
- [45] S. Goffredo, P. Vergni, M. Reggi, E. Caroselli, F. Sparla, O. Levy, Z. Dubinsky, and G. Falini, “The skeletal organic matrix from Mediterranean coral *Balanophyllia europaea* influences calcium carbonate precipitation.” *PLoS One.*, vol. 6, no. 7, p. e22338, 2011.
- [46] M. Reggi, S. Fermani, V. Landi, F. Sparla, E. Caroselli, F. Gizz, Z. Dubinsky, O. Levy, J.-P. Cuif, and Y. Dauphin, “Biomineralization in Mediterranean Corals: The Role of the Intraskelatal Organic Matrix” *Cryst. Growth Des.*, vol. 14, no. 9, pp. 4310–4320, 2014.
- [47] H. Tong, W. Ma, L. Wang, P. Wan, J. Hu, and L. Cao, “Control over the crystal phase, shape, size and aggregation of calcium carbonate via a L-aspartic acid inducing process.” *Biomaterials.*, vol. 25, no. 17, pp. 3923–3929, 2004.
- [48] T. Mass, J. Drake, L. Haramaty, J. Kim, E. Zelzion, D. Bhattacharya, and P. Falkowski, “Cloning and characterization of four novel coral acid-rich proteins that precipitate carbonates in vitro” *Curr. Biol.*, vol. 23, no. 12, pp. 1126–1131, 2013.
- [49] T. Schuler, J. Renkel, S. Hobe, M. Susewind, D. E. Jacob, and M. Panthofer,

- “Designed peptides for biomineral polymorph recognition: a case study for calcium carbonate” *J. Mater. Chem. B*, vol. 2, pp. 3511–3518, 2014.
- [50] W. Zhu, C.-H. Lu, and Feng-Chih Chang, “Supramolecular ionic strength-modulating microstructures and properties of nacre-like biomimetic nanocomposites containing high loading clay” *RSC Adv.*, vol. 2, no. 15, pp. 6295–6305, 2012.
- [51] Y.-B. Hu, M. Wolthers, D. A. Wolf-Gladrow, and G. Nehrke, “Effect of pH and Phosphate on Calcium Carbonate Polymorphs Precipitated at near-Freezing Temperature” *Cryst. Growth Des.*, vol. 15, no. 4, pp. 1596–1601, 2015.
- [52] E. L. Sharp, H. Al-Shehri, T. S. Horozov, S. D. Stoyanov, and V. N. Paunov, “Adsorption of shape-anisotropic and porous particles at the air–water and the decane–water interface studied by the gel trapping technique” *RSC Adv.*, vol. 4, no. 5, pp. 2205–2213, 2014.
- [53] C. Shivkumara, P. Singh, A. Gupta, and M. S. Hegde, “Synthesis of vaterite CaCO₃ by direct precipitation using glycine and l-alanine as directing agents” *Mater. Res. Bull.*, vol. 41, no. 8, pp. 1455–1460, 2006.
- [54] U. Wehrmeister, A. L. Soldati, D. E. Jacob, T. Häger, and W. Hofmeister, “Raman spectroscopy of synthetic, geological and biological vaterite: a Raman spectroscopic study” *J. Raman Spectrosc.*, vol. 41, no. 2, pp. 193–201, 2009.
- [55] U. Wehrmeister, D. E. Jacob, A. L. Soldati, N. Loges, T. Häger, and W. Hofmeister, “Amorphous, nanocrystalline and crystalline calcium carbonates in biological materials” *Amorph. nanocrystalline Cryst. calcium carbonates Biol. Mater.*, vol. 42, no. 5, pp. 926–935, 2010.
- [56] K. Krishnan and R. S. Krishnan, “Raman and infrared spectra of ethylene glycol” *Proc. Indian Acad. Sci. - Sect. A*, vol. 64, no. 2, 1966.
- [57] M. Wahed and E. Mohamed, “Crystallization sequence during evaporation of a high concentrated brine involving the system Na –K–Mg–Cl–SO₄–H₂O” *Desalination*, vol. 355, pp. 11–21, 2015.
- [58] S. R. Dickinson and K. M. McGrath, “Quantitative determination of binary and

tertiary calcium carbonate mixtures using powder X-ray diffraction” *Analyst*, vol. 126, no. 7, pp. 1118–1121, 2001.

- [59] D. Ren, Y. Ma, Z. Li, Y. Gao, and Q. Feng, “Hierarchical structure of asteriscus and in vitro mineralization on asteriscus substrate.” *J. Cryst. Growth*, vol. 325, no. 1, pp. 46–51, 2011.

- [60] A. Sellinger, P. M. Weiss, A. Nguyen, Y. Lu, R. A. Assink¹, W. Gong, and J. Brinker, “Continuous self-assembly of organic–inorganic nanocomposite coatings that mimic nacre” *Nature*, vol. 394, pp. 256–260, 1998.

- [61] J. Li, D. Liu, B. Li, J. Wang, S. Han, L. Liu^{ab}, and H. Wei, “A bio-inspired nacre-like layered hybrid structure of calcium carbonate under the control of carboxyl graphene” *CrystEngComm*, vol. 17, no. 3, pp. 520–525, 2015.

Annex

Annex 1

Table A1. 1: Solution parameters tested

CaCl ₂ .2H ₂ O (mmol) +50mL ethylene glycol	NaHCO ₃ (mmol)+ 50mL ethylene glycol	Temperature ©	Reaction time (min)	Rotation speed (rpm)	Method
5	10	40	2		Ultra-sound bath
			5		
			10		
			30		
			60		
CaCl ₂ .2H ₂ O (mmol) +50mL ethylene glycol	NaHCO ₃ (mmol)+ 50mL ethylene glycol	Temperature ©	Reaction time (min)	Rotation Speed (rpm)	Method
5	10	40	5	400 e 800	Oil bath
			10		
			30		
			60		
			120		
			24 hours		
		75	5		
			10		
			30		
			60		
			120		
5	5	40	30	400	
	15				
	20				
	30				
5	20	75			
	25				

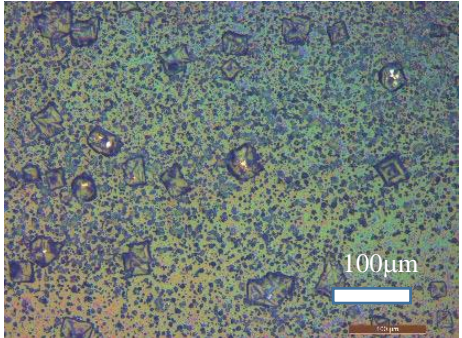
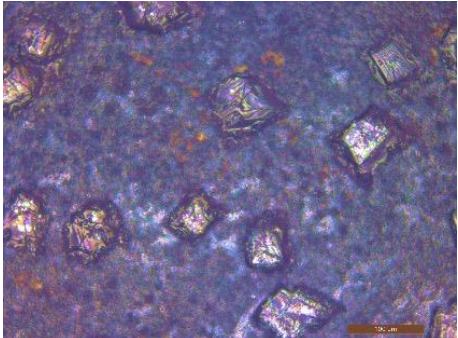
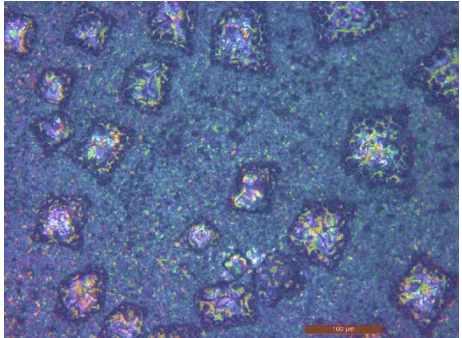
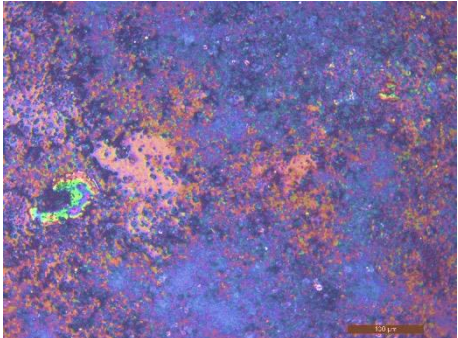
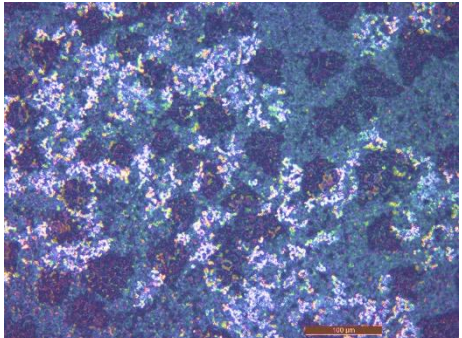
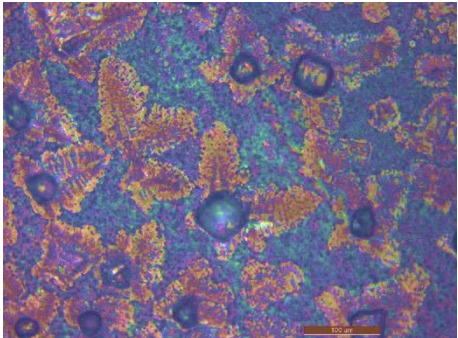
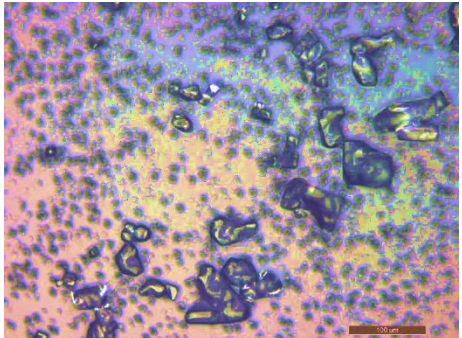
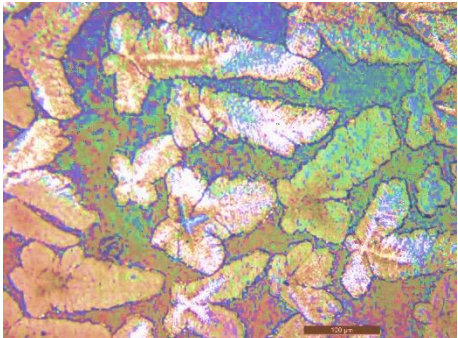
Table A1. 2: Dip-coating parameters used

Speed	Cycles	Temperature	Dip	Dry	In-between cup
500 um/s	3	22°C	1 min	3 min	
	5				
	10				
500um/s	3	40°C	1 min	3 min	
	5				
	10				
500um/s	3	40°C	3 min	3 min	
	5				
	10				
500um/s	3	40°C	5 min	3 min	
	5				
	10				
5mm/s	3	22°C	3 min	1 seg	
	5				
	10				
5mm/s	3	40°C	3 min	3 min	
	5				
	10				
5mm/s	3	40°C	3 min	1 seg	
	5				
	10				
5mm/s	10	22°C	3 min	3 min	Water/2 sec
	20				
5mm/s	10	22°C	10 min	3 min	Water/2 sec
5mm/s	5	22°C	1 min	3 min	Acetone/2 sec
	10				
	20				
5mm/s	5	22°C	10 seg	3 min	Acetone/2 sec
	10				
	20				
5mm/s	5	22°C	10 seg	3 min	Methanol/PVP/2 min
	10				
	15				
	20				
5mm/s	5	22°C	10 seg	3 min	Methanol/PVP/2 min
	10				
	15				
	20				
CaCO ₃ /PVP					

5mm/s	5	22°C	10 seg	3 min	Methanol/PVP/2 min
	10				
	15				
	20				
Ca/Sea Water/PVP					
5mm/s	5	22°C	10 seg	3 min	Methanol/PVP/2 min
	10				
	15				
	20				

Annex 2

Table A2. 1: Influence of time and temperature for a solution with magnetic stir at 400rpm.

Time	400 rpm	
	40°C	75°C
5 min		
10 min		
30 min		
60 min		

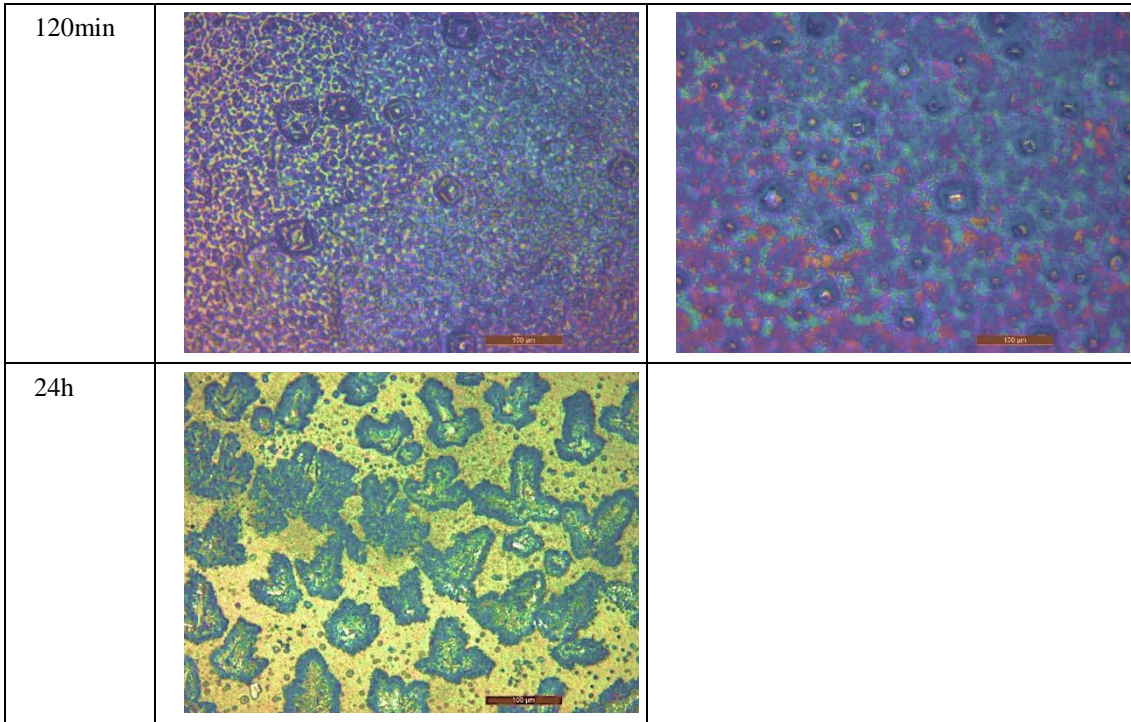
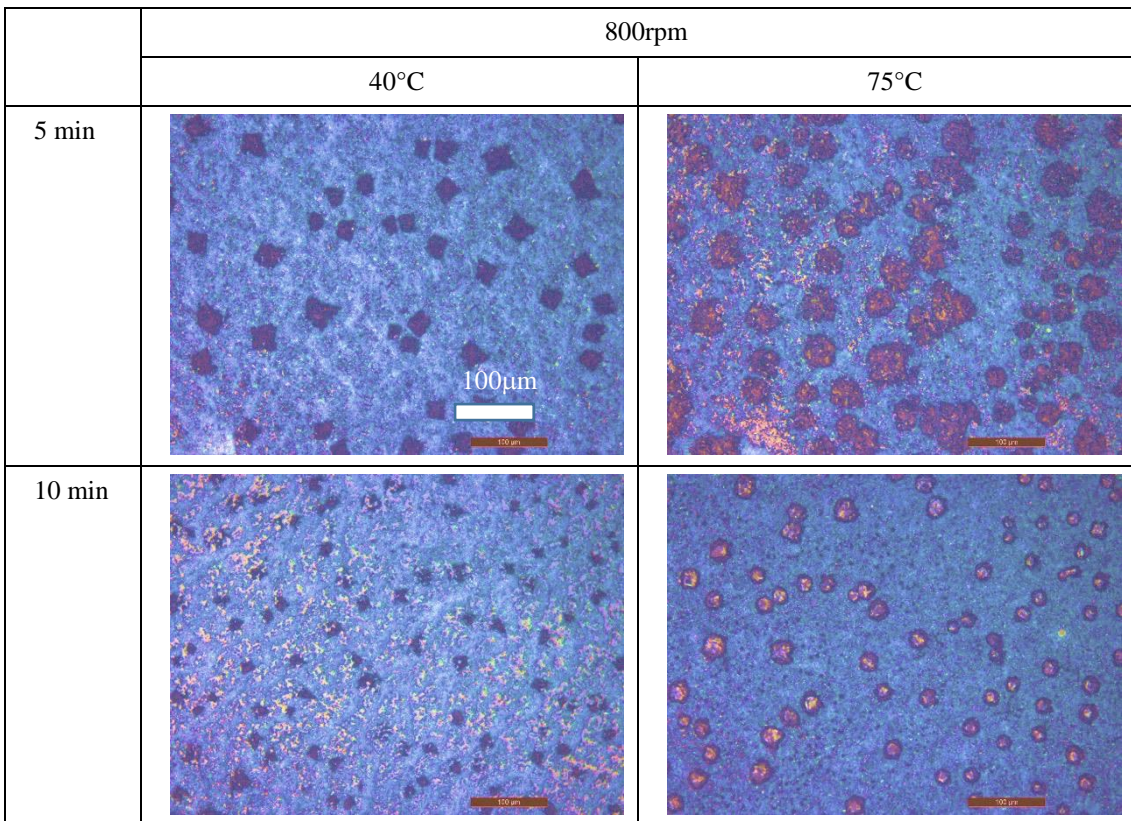


Table A2. 2: Influence of time and temperature for a solution with magnetic stir at 800rpm.



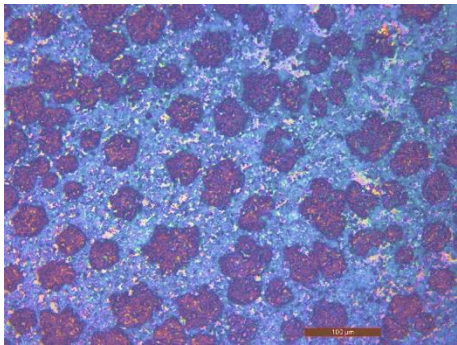
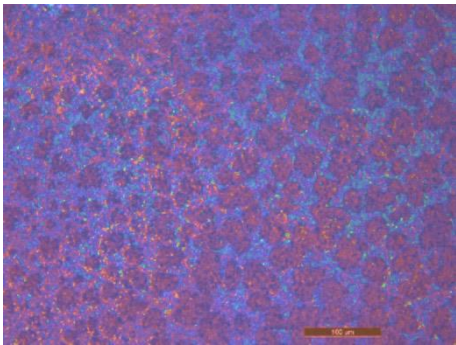
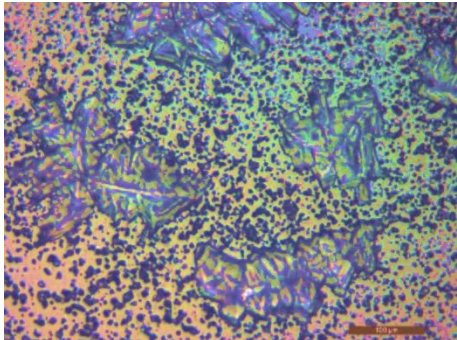
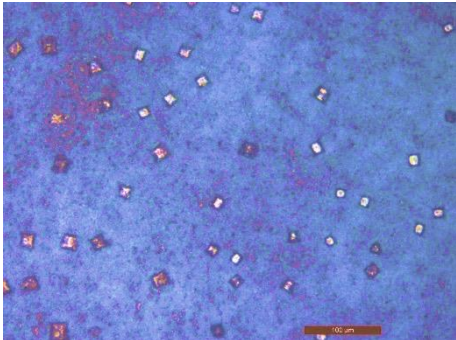
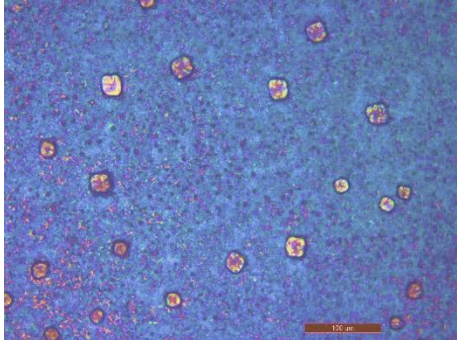
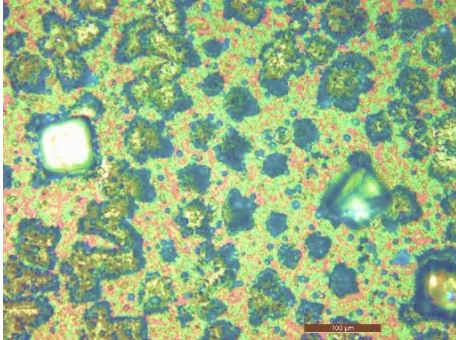
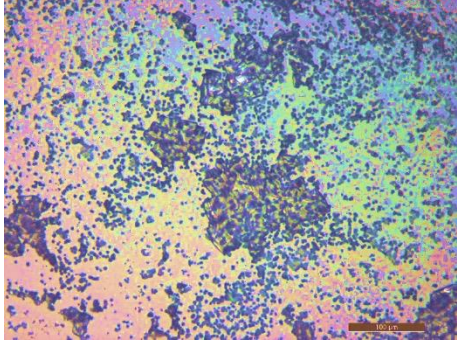

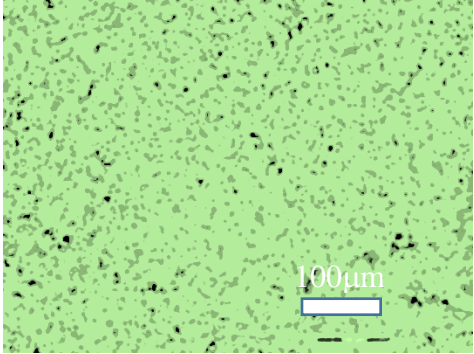
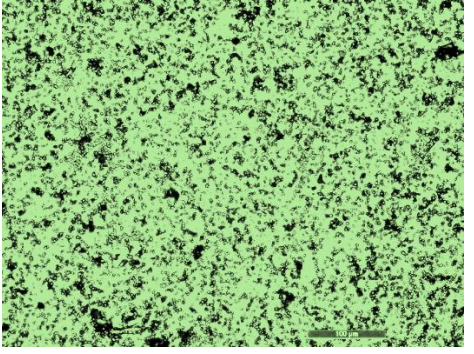
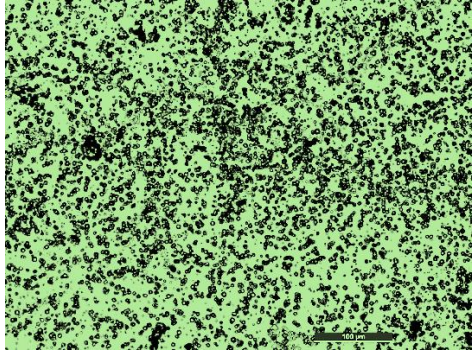
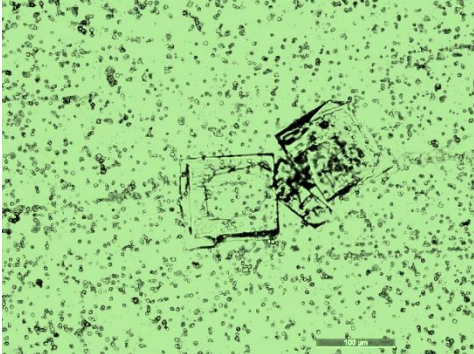
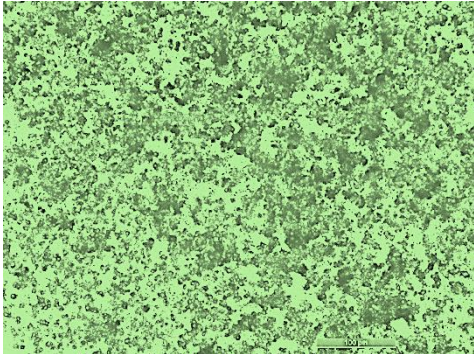
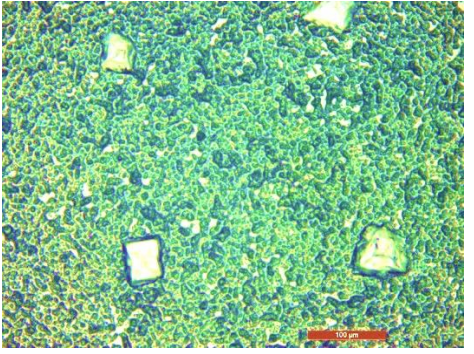
30 min		
60 min		
120 min		
24h		

Table A2. 3: Influence of time and temperature for a solution without magnetic stir.

		No magnetic stir	
		10 min	30 min
10°C			
		60 min	120min
			
		40°C	T _{amb} (dried at 70°C)
120 min			
		75°C	

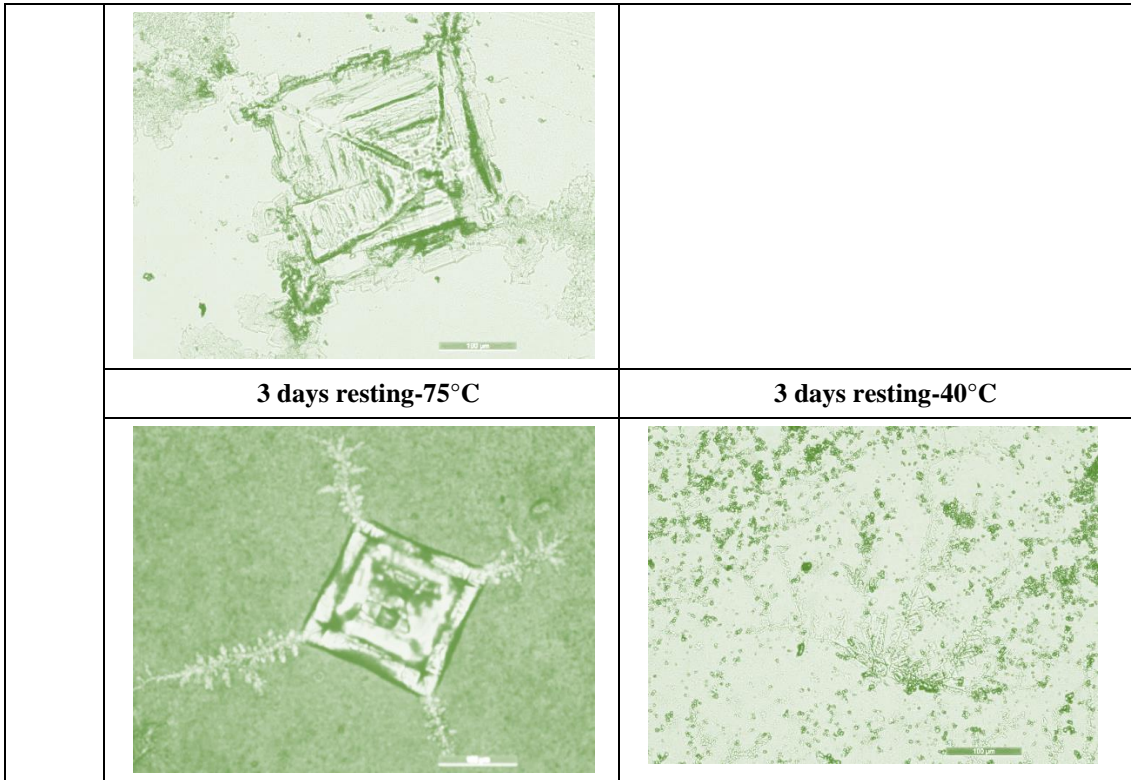
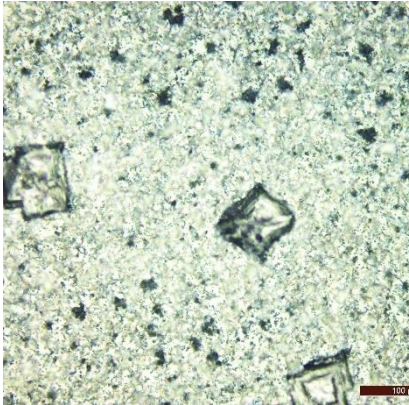
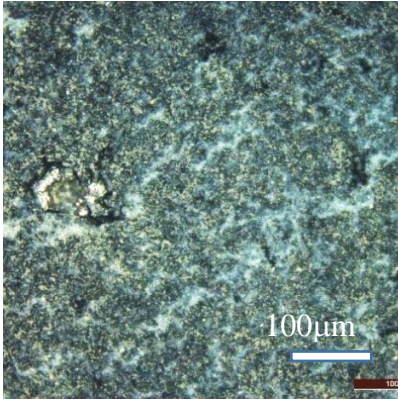
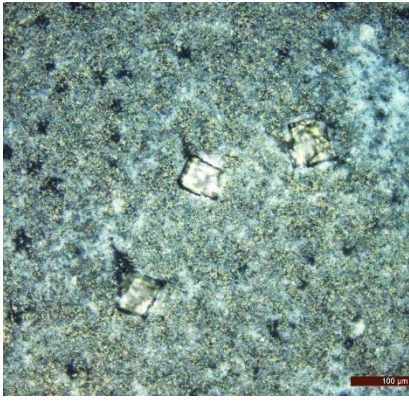
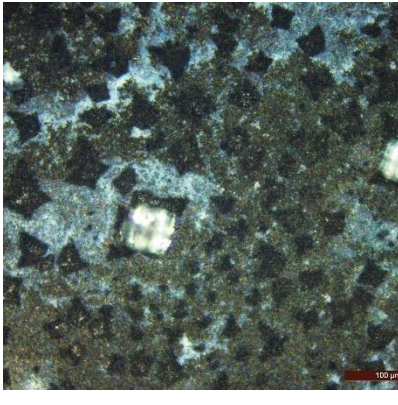



Table A2. 4: Influence of the ultra-sounds in the solution

Ultra-sounds 40°C			
2 min		5 min	
10 min		30 min	
60 min			

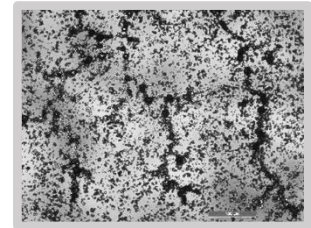
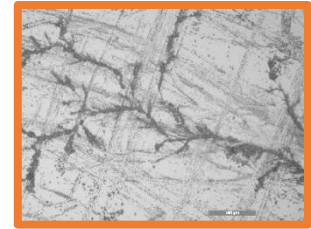
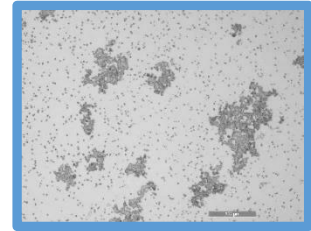
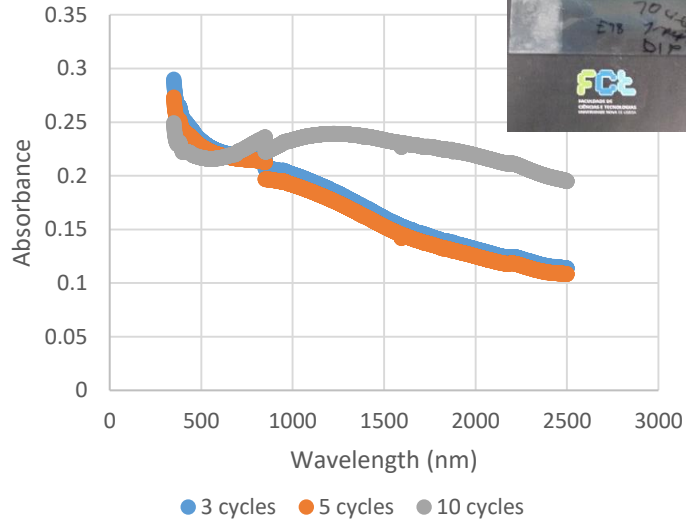
Annex 3

Table A3. 1: Influence of dip parameters and dip cycles in the transmittance of samples with the respective images of films taken in the microscope.

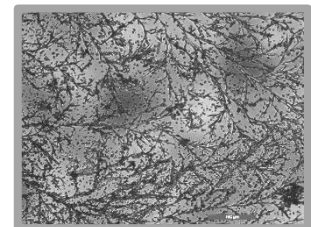
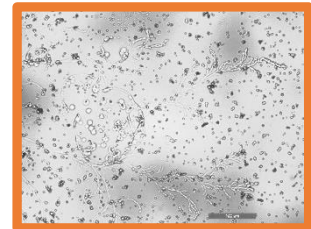
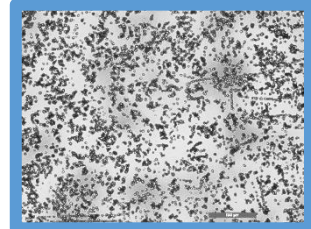
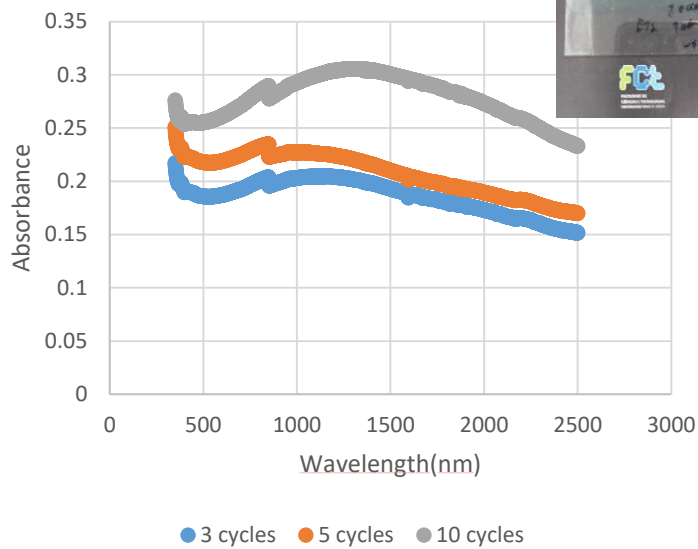
Influence of dip velocity																													
<p style="text-align: center;">T 40°C, 500um/s, 3 min Dip, 3 min Dry</p> <table border="1"> <caption>Approximate Absorbance values for 500um/s</caption> <thead> <tr> <th>Wavelength (nm)</th> <th>3 cycles (blue)</th> <th>5 cycles (orange)</th> <th>10 cycles (grey)</th> </tr> </thead> <tbody> <tr><td>400</td><td>0.25</td><td>0.28</td><td>0.28</td></tr> <tr><td>500</td><td>0.20</td><td>0.26</td><td>0.25</td></tr> <tr><td>1000</td><td>0.16</td><td>0.25</td><td>0.28</td></tr> <tr><td>1500</td><td>0.12</td><td>0.22</td><td>0.29</td></tr> <tr><td>2000</td><td>0.09</td><td>0.19</td><td>0.27</td></tr> <tr><td>2500</td><td>0.08</td><td>0.16</td><td>0.22</td></tr> </tbody> </table> <p style="text-align: center;">● 3 cycles ● 5 cycles ● 10 cycles</p>	Wavelength (nm)	3 cycles (blue)	5 cycles (orange)	10 cycles (grey)	400	0.25	0.28	0.28	500	0.20	0.26	0.25	1000	0.16	0.25	0.28	1500	0.12	0.22	0.29	2000	0.09	0.19	0.27	2500	0.08	0.16	0.22	
Wavelength (nm)	3 cycles (blue)	5 cycles (orange)	10 cycles (grey)																										
400	0.25	0.28	0.28																										
500	0.20	0.26	0.25																										
1000	0.16	0.25	0.28																										
1500	0.12	0.22	0.29																										
2000	0.09	0.19	0.27																										
2500	0.08	0.16	0.22																										
<p style="text-align: center;">T 40°C, 5mm/s, 3 min Dip, 3 min Dry</p> <table border="1"> <caption>Approximate Absorbance values for 5mm/s</caption> <thead> <tr> <th>Wavelength (nm)</th> <th>3 cycles (blue)</th> <th>5 cycles (orange)</th> <th>10 cycles (grey)</th> </tr> </thead> <tbody> <tr><td>400</td><td>0.22</td><td>0.28</td><td>0.52</td></tr> <tr><td>500</td><td>0.18</td><td>0.26</td><td>0.55</td></tr> <tr><td>1000</td><td>0.16</td><td>0.28</td><td>0.50</td></tr> <tr><td>1500</td><td>0.13</td><td>0.25</td><td>0.40</td></tr> <tr><td>2000</td><td>0.11</td><td>0.22</td><td>0.30</td></tr> <tr><td>2500</td><td>0.10</td><td>0.18</td><td>0.22</td></tr> </tbody> </table> <p style="text-align: center;">● 3 cycles ● 5 cycles ● 10 cycles</p>	Wavelength (nm)	3 cycles (blue)	5 cycles (orange)	10 cycles (grey)	400	0.22	0.28	0.52	500	0.18	0.26	0.55	1000	0.16	0.28	0.50	1500	0.13	0.25	0.40	2000	0.11	0.22	0.30	2500	0.10	0.18	0.22	
Wavelength (nm)	3 cycles (blue)	5 cycles (orange)	10 cycles (grey)																										
400	0.22	0.28	0.52																										
500	0.18	0.26	0.55																										
1000	0.16	0.28	0.50																										
1500	0.13	0.25	0.40																										
2000	0.11	0.22	0.30																										
2500	0.10	0.18	0.22																										

Influence of temperature

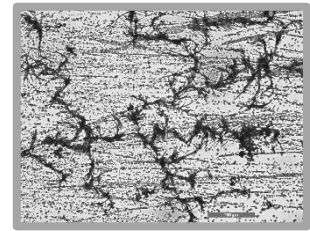
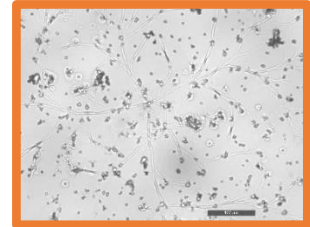
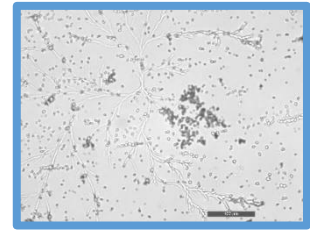
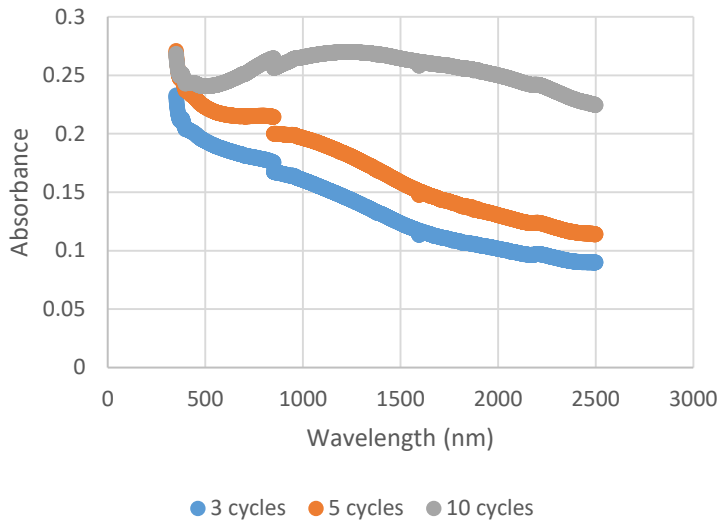
T ambiente (22°C), 500um/s,
1min Dip, 3 min Dry



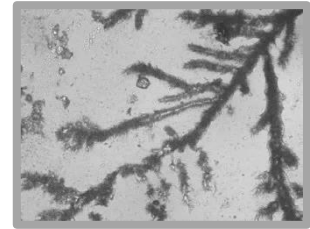
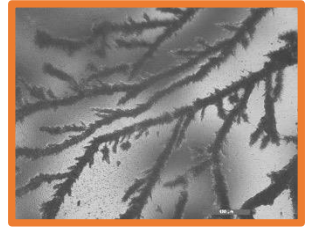
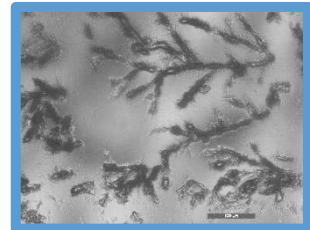
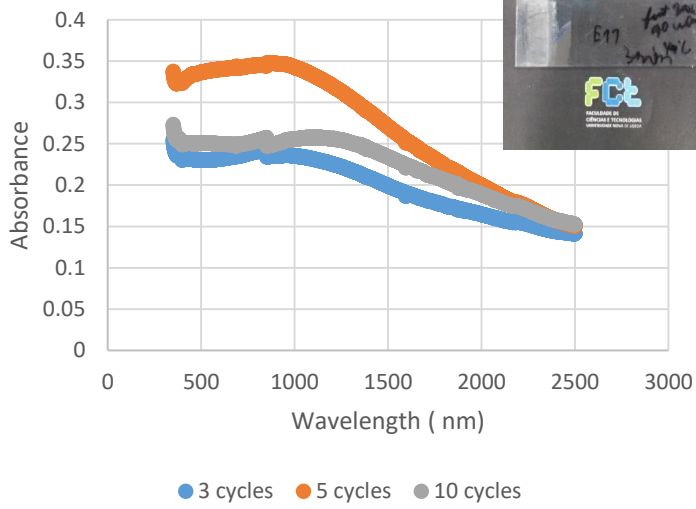
T 40°C, 500um/s, 1 min Dip,
3 min Dry

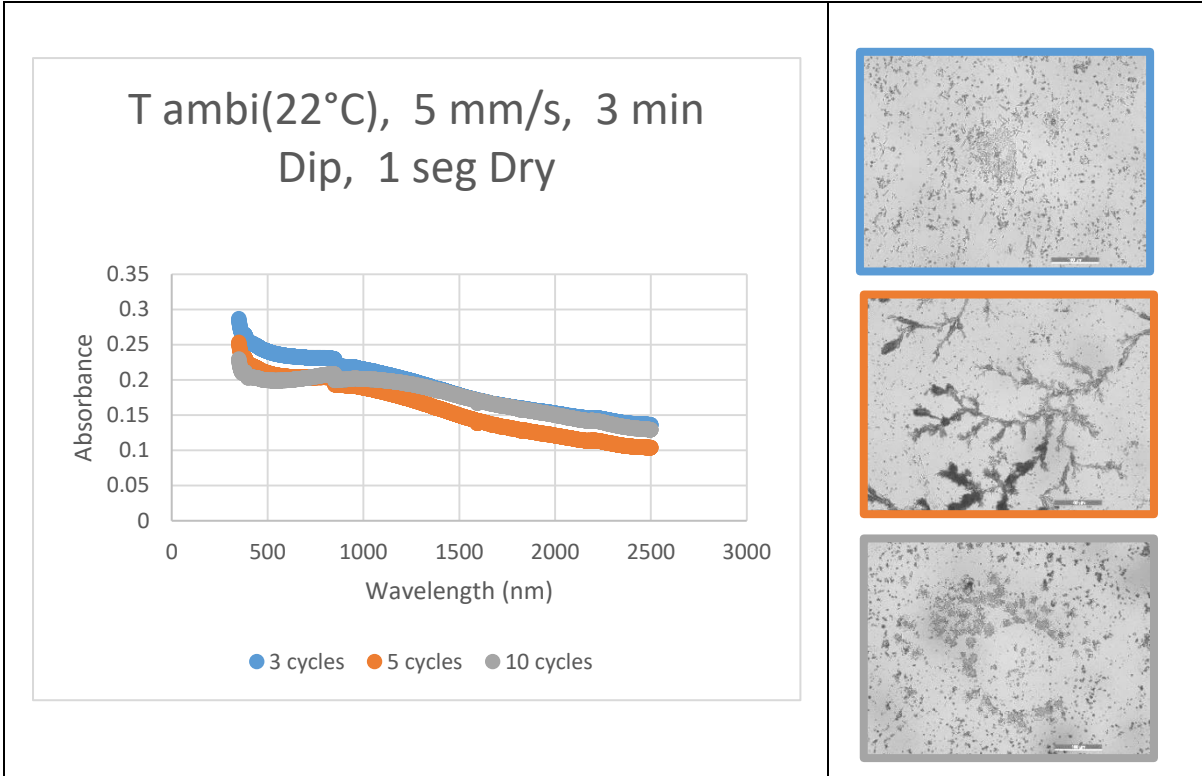


T 40°C, 500um/s, 5 min Dip,
3 min Dry

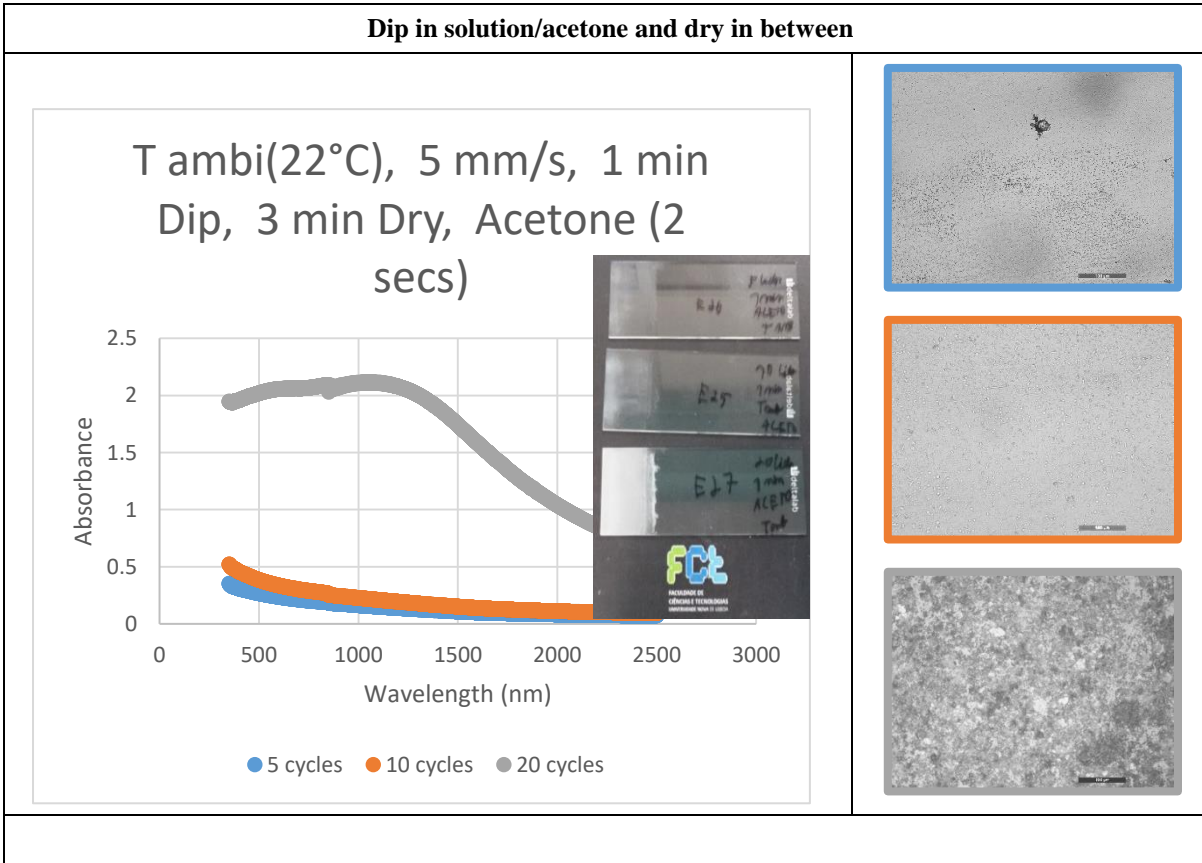


T 40°C, 5 mm/s,
3min Dip, 1 seg Dry



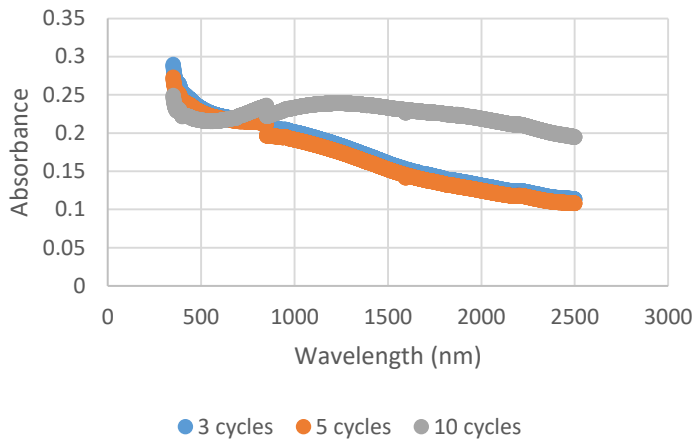


Cycles variation

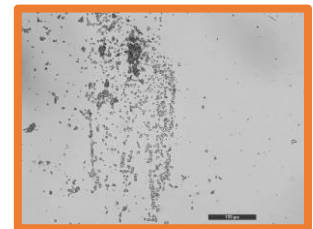
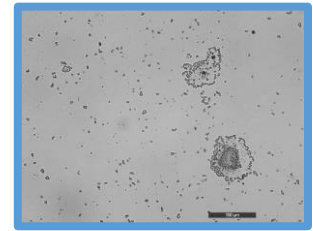
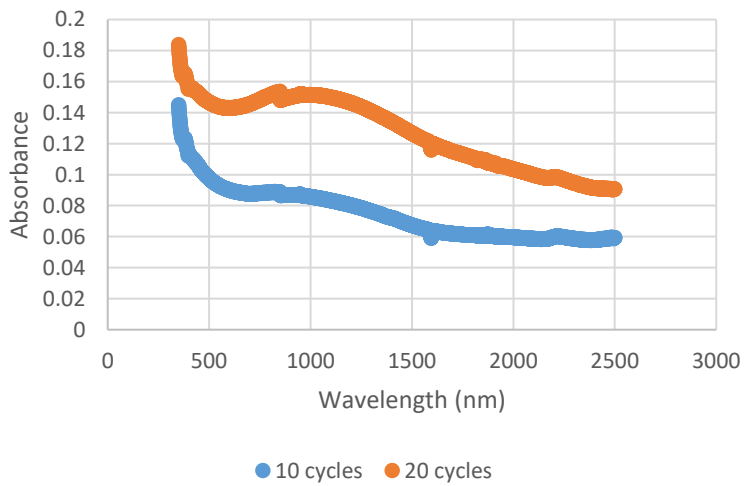


Dry in air

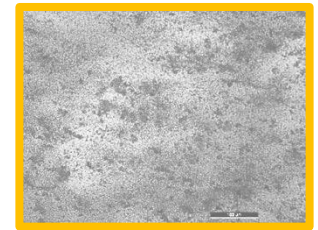
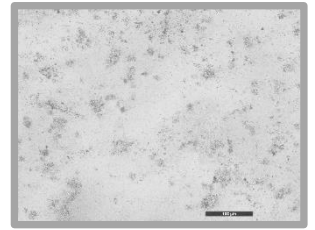
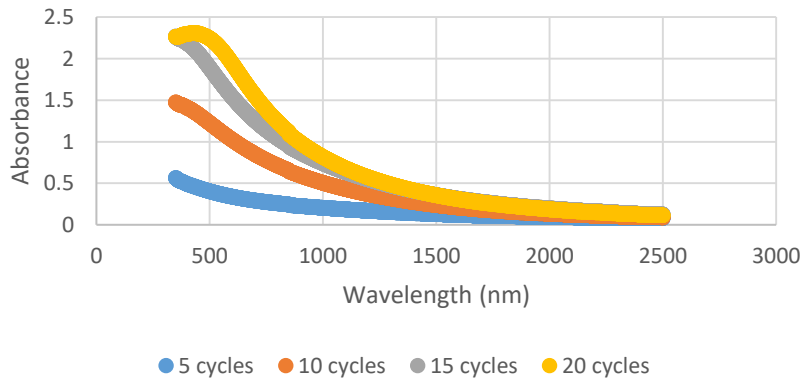
T ambiente (22°C), 500um/s,
1minute Dip, 3 minutes Dry



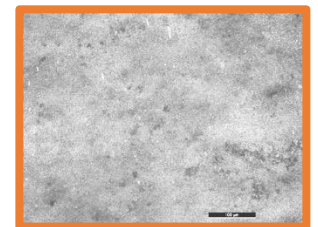
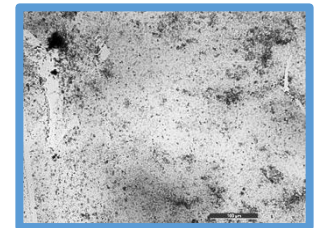
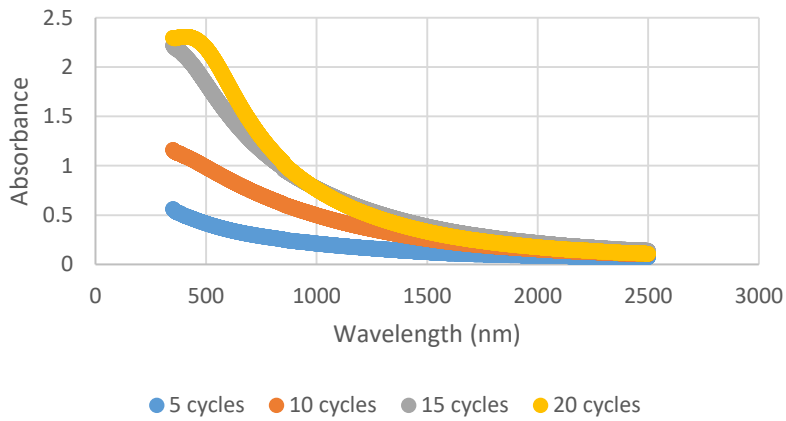
T ambi(22°C), 5mm/s, 3min
Dip, 1 seg Dry, Water(2 secs)



CaCl₂/NaHCO₃/PVP
 Metanol/PVP 2min, 3 min dry,
 5 mm/s, T amb (27°C), 10 seg dip

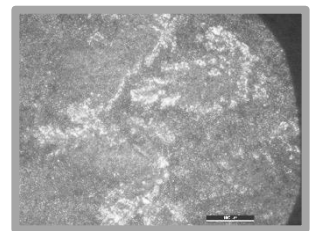
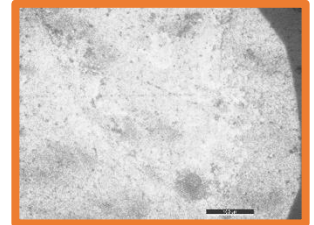
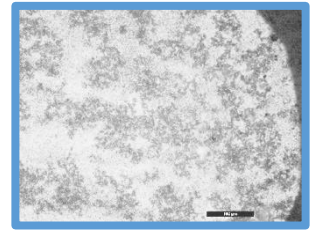
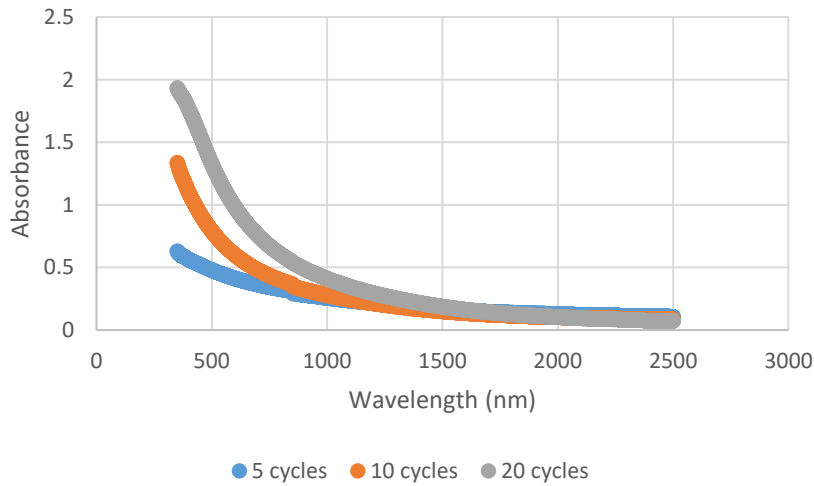


CaCl₂/NaHCO₃/PVP 150°C 1 hour
 Metanol/PVP 2min, 3 min dry,
 5 mm/s, T amb (27°C), 10 seg dip



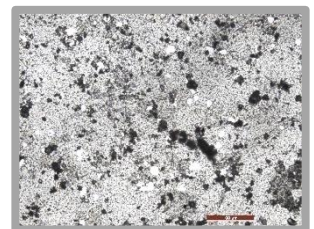
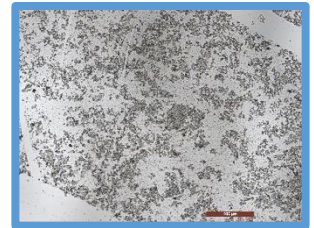
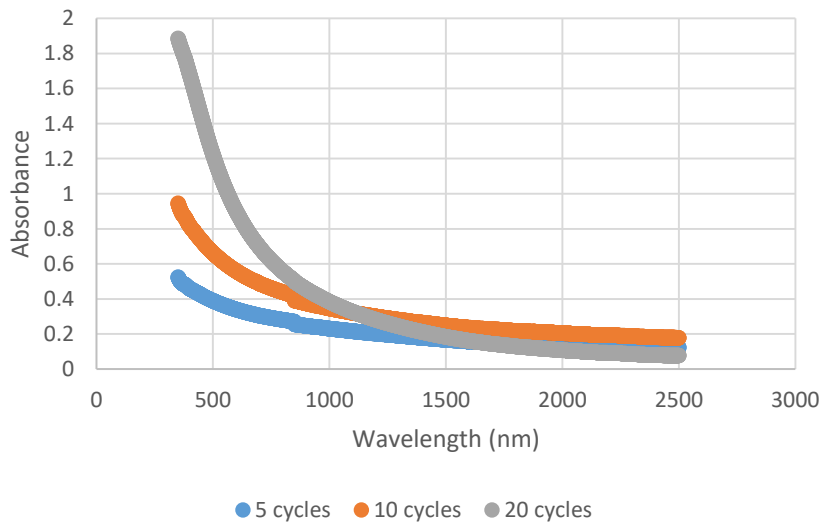
CaCl₂/PVP/NaHCO₃/PVP

Metanol/PVP 2min, 3 min dry,
5 mm/s, T amb (27°C), 10 seg dip

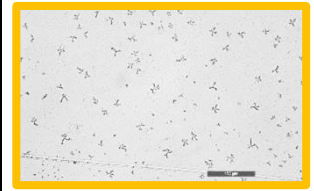
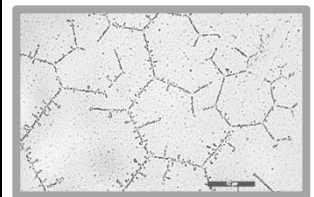
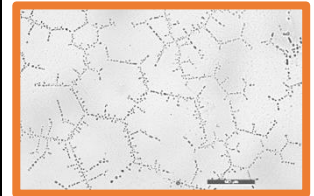
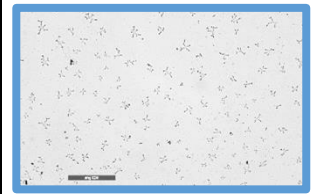
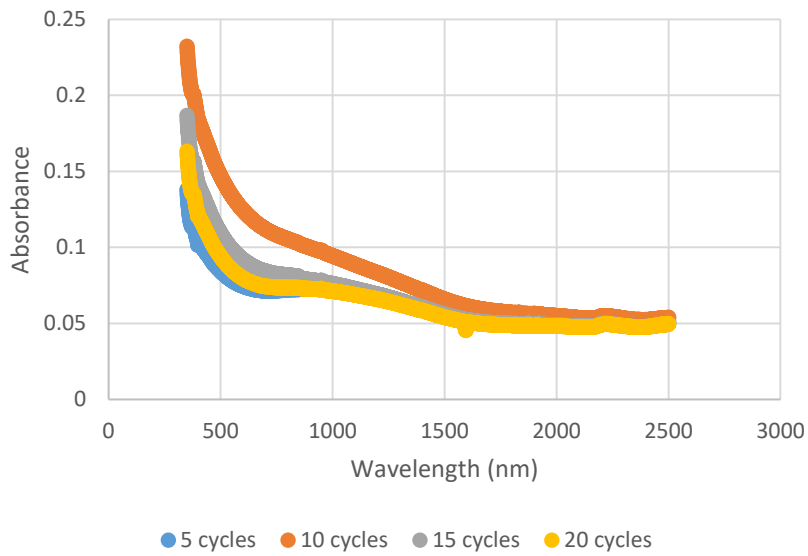


CaCl₂/PVP/NaHCO₃/PVP 150°C 1hour

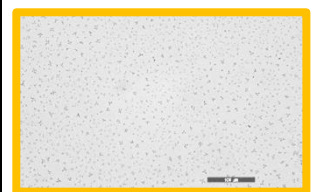
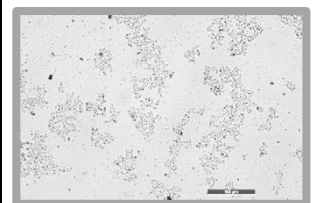
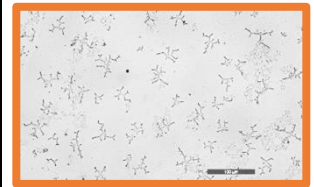
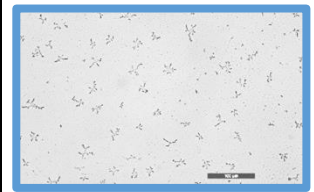
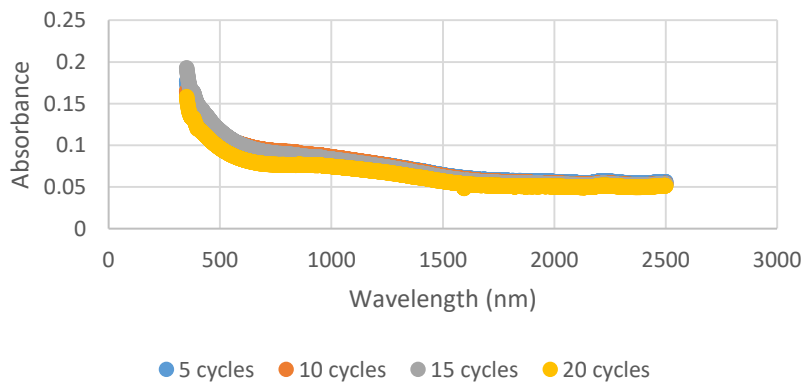
Metanol/PVP 2min, 3 min dry,
5 mm/s, T amb (27°C), 10 seg dip



CaCO₃/PVP Metanol/PVP 2min, 3 min dry, 5 mm/s, T amb (27°C), 10 seg dip



CaCO₃/PVP 150°C 1hour
Metanol/PVP
 2min, 3 min dry, 5 mm/s, T amb (27°C), 10 seg dip



Ca/Sea Water/PVP

Metanol/PVP 2min, 3 min dry, 5
mm/s, T amb (27°C), 10 seg
dip

